2012

Adaptive sliding mode control for energy management of DC power using fuel cells and ultracapacitors

Roshini Sukanya Ashok Kumar

ADAPTIVE SLIDING MODE CONTROL FOR ENERGY MANAGEMENT OF DC POWER USING FUEL CELLS AND ULTRACAPACITORS

by

ROSHINI SUKANYA ASHOK KUMAR

A THESIS

Submitted in partial fulfillment of the requirements
for the degree of Master of Science
in
The Department of Electrical and Computer Engineering
to
The School of Graduate Studies
of
The University of Alabama in Huntsville

HUNTSVILLE, ALABAMA

2012

In presenting this thesis in partial fulfillment of the requirements for a Master's degree from The University of Alabama in Huntsville, I agree that the Library of this University shall make it freely available for inspection. I further agree that permission for extensive copying for scholarly purposes may be granted by my advisor or, in his/her absence, by the Chair of the Department or the Dean of the School of Graduate Studies. It is also understood that due recognition shall be given to me and to The University of Alabama in Huntsville in any scholarly use which may be made of any material in this thesis.

Rashmi Sukanya Ashok Kumar 02/28/12

(Student signature) (Date)

THESIS APPROVAL FORM

Submitted by Roshini Sukanya Ashok Kumar in partial fulfillment of the requirements for the degree of Master of Science in Engineering is accepted on behalf of the Faculty of the School of Graduate Studies by the thesis committee.

We, the undersigned members of the Graduate Faculty of The University of Alabama in Huntsville, certify that we have advised and/or supervised the candidate on the work described in this thesis. We further certify that we have reviewed the thesis manuscript and approve it in partial fulfillment of the requirements for the degree of Master of Science in Engineering.

Yun Stutesell 02/28/2012 Committee Chair

(Date)

Laurie J. Yoon 2/28/12 Committee Member

(Date)

Mark Tiek 3/9/12 Committee Member

(Date)

Carol Gwaltney for Dr. Lindquist 3/12/12 Department Chair

(Date)

Gregory Hale 03/14/12 College Dean

(Date)

Rhonda Kay Gaede 4/2/12 Graduate Dean

(Date)

ABSTRACT
The School of Graduate Studies
The University of Alabama in Huntsville
Degree Master of Science in Engineering College/Dept. Engineering/Electrical and Computer Engineering.

Name of Candidate: Roshini Sukanya Ashok Kumar

Title ADAPTIVE SLIDING MODE CONTROL FOR ENERGY MANAGEMENT OF DC POWER USING FUEL CELLS AND ULTRACAPACITORS

This thesis deals with controlling autonomous electric power system that comprises Proton Exchange Membrane fuel cell (PEMFC) that is considered as a primary source of electrical energy, the DC-DC boost power converter, and the ultra capacitor. System's PEMFC/ultra capacitor/DC-DC boost power converter zero dynamics are analyzed and appeared to be stable. Relative degree approach is applied for direct control of the output load voltage, the fuel cell and ultra capacitor current/voltage in the presence of the model uncertainties. The sliding mode observer is employed for identification of the load resistance, which estimated value is used for generating the fuel cell/ultra capacitor current command profile. The adaptive gain super-twisting sliding mode controller controls the current in PEMFC. The decoupled traditional SMCs are designed for controlling the output voltage and the fast component of the load current or voltage of the ultra capacitor. The efficacy and robustness of the proposed three-fold SMC and 2-SMC adaptive-gain controllers are confirmed via computer simulations.

Abstract Approval: Committee Chair Yuri Shtessel 02/28/2012

Department Chair Qun Zhang for Dr. Lindquist 3/12/12

Graduate Dean Rhonda Kay Saede 4/2/12

ACKNOWLEDGMENTS

The work described in this thesis would not have been possible without the assistance of a number of people who deserve special mention. First, I would like to thank Dr. Yuri Shtessel for his suggestion of the research topic and his guidance throughout all the stages of the work. His advice and patient support were invaluable during the construction of this work. I would like to thank my family and my friends who encouraged me to begin work on this degree and who helped me to complete this work. Thank you.

TABLE OF CONTENTS

CHAPTER1

INTRODUCTION

Fuel cells are now on the verge of being introduced commercially, revolutionizing the way we presently produce and store power. In this thesis, hydrogen is used as a fuel, offering the prospect of supplying the world with clean, sustainable electrical power. Fuel cells, a promising next-generation power source, are widely used in both automotive and stationary applications due to their high power density and low emissions. Fuel cells play a vital role because they offer an alternative environmental friendly fuel for transportation, which reduces the amount of the air pollution and thereby minimizing the risk of global warming. Fuel cells, is a form of green technology, as they are able to produce power for electric motors or in place of generators, they have been successfully used to replace gasoline engines. The fact that the byproducts of the chemical reactions involved in producing energy create water and some heat makes fuel cells a better option as compared to what is produced in combustion of other fuels. The green energy cars powered by the fuel cells are now replacing the gasoline powered engines. Fuel cells find their applications in most stationary and mobile applications, and are also used in conjunction with other power conditioning converters. A circuit model of the entire fuel cell system would be beneficial; especially in power electronics for designing converters associated with the fuel cell for various load applications [3,4].Fuel cells also help designing the energy efficient buildings. Application of fuel cells in industries using enormous amount of power can increase the efficiency by reducing the power consumption. The Fig.1 shows the application of fuel cell system being installed in a car and also in households.

Implementation of Fuel Cell in a Car

Implementation of Fuel Cell in a Household

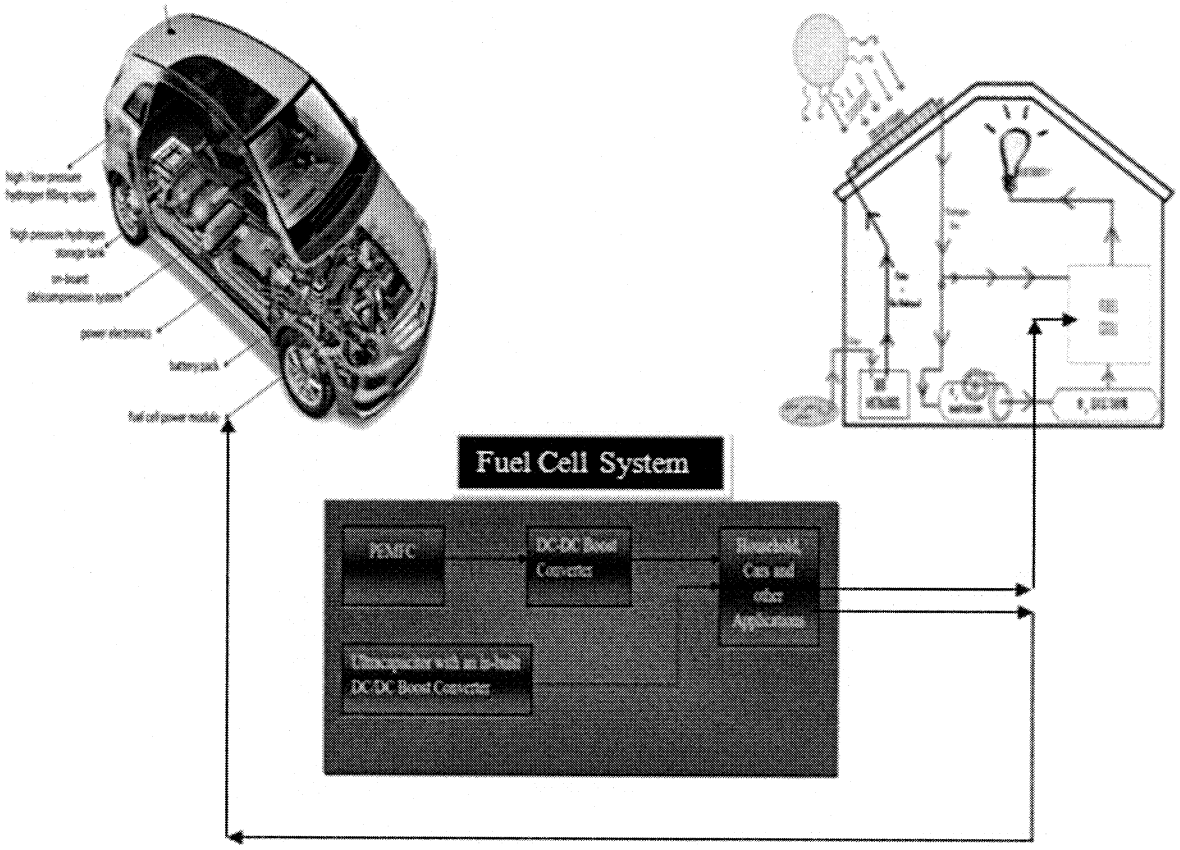

Fig.1 Applications of Fuel Cell System

A Proton Exchange Membrane Fuel Cell (PEMFC) that is in the core of the Fuel Cell System (Fig. 1) is an electrochemical device in which the electrochemical reaction is converter directly into electricity by combining hydrogen fuel with oxygen from the air with the heat as the bypass [1].This thesis elaborates and resolves the coordination and feedback control problem of the fuel cell system involving the PEMFC associated with an impulse energy source, the ultra capacitors (UCs) when applied to high instantaneous

dynamic power systems. Systems of PEMFC/DC-DC power converter/Ultra capacitor can serve as an emergency source of energy in the event of long term power outage or as an electric power supply unit for cars and other autonomous vehicles. The rapid voltage drop and a slow response to the load demand is one of the critical issues faced by the PEMFC. This critical issue is resolved by using the energy storage devices like the ultra capacitors and the power regulation devices like the DC/DC converters. These devices are required to work along with the PEMFC in order to provide regulated and fast response power to a variable load. A typical PEMFC-Ultra capacitor system consists of a PEM fuel cell stack as the main power source, a boost DC/DC converter as the power conditioning device and an Ultra capacitor, which is implemented as an energy management or an auxiliary power source. This hybridization of the fuel cell system is considered as the electrical power unit, while being used in the cars and other autonomous vehicles, it provides increased durability and safer performance especially in shut-down and start-up modes. Usually [3], the fuel cell is controlled separately and power conditioned later. This is mainly due to the uncertainties in varying of pressure and their disability to accommodate to these changes. The control challenges faced by the fuel cell system are –

- Controlling the pressure variation of oxygen/hydrogen
- Disability to control the fast charge and discharge modes
- Increasing the efficiency of the DC-DC converter by using highly effective robust control techniques

- Accurate stabilization of the output voltage in the presence of the system parametric uncertainties, including rapid changes of the load

Sliding Mode Control is used in this work as the control tool for controlling the fuel cell system. Sliding mode control (SMC) is one of the powerful control strategies to deal with uncertain control systems [5-7]. The main feature of SMC is the robustness against parameter variations and external disturbances. The system model parameters are not precisely known and environmental disturbance is quite difficult to determine. Insensitivity to matched external disturbances and to matched parameter variations have become the benchmark of SMC systems. Higher Order Sliding Mode (HOSM) control is used to conserve the same properties of SMC and also to limit the chattering effect and increase stabilization accuracy. Sliding mode control with gain adaptation retains the main properties of SMC and can control the system with matched bounded disturbances, in which the bounds are unknown. Using adaptive gain SMC and HOSM allows reducing the control chattering. The 2-SMC algorithm with gain adaptation is used in this thesis to control PEMFC.

The objective of the thesis is to control the power system that comprises three controlled components: PEMFC, an ultra capacitor and a boost DC-DC power converter, in the presence of model uncertainties using sliding mode control techniques.

The structure of the thesis is as follows.

Chapter 2 elaborates the physical description and the working principle of the PEMFC in detail. The need for PEMFC and its preference over the other types of the fuel cells is also briefly summarized.

Chapter 3 focuses mainly on the boost DC-DC converter, in which the output voltage is controlled directly. In this chapter, the different types of DC-DC converters are studied and their significance of usage in this fuel cell system is elucidated.

Chapter 4 explains the performance and necessity of the energy management device (Ultra capacitor) and also explains the vitality of UC in the field of green technology.

Chapter 5 derives the combined math model of the Fuel Cell/Ultra capacitor/ DC-DC boost converter system using the equations of chapters 2, 3 and 4.The control problem is formulated.

Chapter 6 unfolds the concept of sliding mode control. Different types of Sliding mode controls are studied and analyzed, in order to choose the control appropriately for the various components of fuel cell system. The sliding mode observer is employed for identification of the load resistance, whose estimated value is used for generating the fuel cell/ultra capacitor current command profile. The simulation results of various controls are studied for better understanding of operations of various sliding mode control techniques.

Chapter 7 is the backbone of the entire thesis, since it elaborates the controller design for the Fuel cell System. Relative degree approach is applied for direct control of the output load voltage, the fuel cell and ultra capacitor current/voltage in the presence of the model uncertainties. Adaptive second order super-twisting control, in terms of the oxygen pressure, is used to control the PEMFC current. Traditional sliding mode controllers control the DC-DC boost power converter and the ultra capacitor in a charge/discharge mode.

Chapter 8shows the simulation results of the fuel cell system dynamics as derived in chapter 5. The theoretical results are verified with the simulation results. The comparative study of the simulated and theoretical values are analyzed and rectified accordingly.

Chapter 9 summarizes the results of the thesis and draws a conclusion.

Chapter 10 includes the references.

Chapter 2

PHYSICAL DESCRIPTION AND MATH MODELING OF PEMFC

2.1 Overview of Fuel Cell Technology

There are currently six main types of fuel cells: Proton Exchange Membrane (PEMFC), Direct Methanol (DMFC), Alkali (AFC), Phosphoric Acid (PAFC), Solid Oxide (SOFC) and Molten Carbonate (MCFC). All of these types share the same basic theory of operation but are very different in their construction and applications [4].

Types of Fuel Cell	Efficiency	Operating Temperature	Applications
Polymer electrolyte membrane (PEMFC)	40% - 80% with Combined heat and power(Cogeneration)	175° F (80°C)	Transportation – cars, buses, boats, trains, scooters, bikes and trucks Residential – household electrical power needs Portable – laptop computers, cell phones, medical equipment.
Direct methanol (DMFC)	40%	120 - 150° F(50-80°C)	Portable – cell phones, laptop computers, vacuum cleaners, highway road signs
Alkali(AFC)	60-80%	250-500°F(120-260°C)	Space Vehicles
Phosphoric acid(PAFC)	40-80%	300-400°F(148-205°C)	Waste water management-Generates power from methane gas
Solid oxide(SOFC)	55-85%	1800°F(982°C)	Commercial purposes like office buildings, hospitals, hotels and airport terminals
Molten Carbonate(MCFC	55-85%	1200°F(650°C)	Commercial purposes like office buildings, hospitals,

Fig:2 Comparative study of various types of Fuel Cells

The Fig.2 illustrates the comparative study of the six different types of fuel cells. The thesis mainly focuses on the PEM Fuel cell. The most attractive fuel is hydrogen as it does not produce any harmful byproducts, only water. This allows oxygen to be used as the oxidant, which is readily available in the atmosphere [5]. Inside a fuel cell, there are three layers, the anode, electrolyte and the cathode. Each type of fuel cell uses different materials for each of these layers, but the basic operating principle remains the same. The fuel is injected into the anode side and is reduced to positive ions and free electrons by the anode. The free electrons flow in the opposite of the positive ions, exit the cell and are used by external circuitry to provide power. The positive ions flow through the electrolyte and when they reach the cathode, they are reduced through another chemical reaction with the oxidant. This reaction recombines the positive ions with the free electrons that return from the external circuitry [4].

Theoretically, one of these cells can produce around 1.18V [6], but when under load, the voltage drops to around 0.7V [5]. At such a low voltage, it is hard to harness the power for residential consumption. To solve this multiple cells are stacked in series, effectively increasing the voltage and the power.

The general efficiency of fuel cell systems is in the range of 40-50% and can be increase up to 85% by using excess heat and steam to drive turbines for cogeneration of electricity [7]. Along with efficient and reliable operation, fuel cells have drastically reduced emissions of greenhouse gases and other harmful hydrocarbons. The fact, that they are relatively quite as compared to a power plant, allows them to be located on-site residential areas or near businesses [4].

PEMFC is preferred over the types of the fuel cells. Proton Exchange Membrane (PEM) Fuel Cells emit no pollutants and have high energy efficiency and power density. Coupled with its low operating temperature and the resulting quick startup of power generation, these factors make PEM Fuel Cells an ideal power source for a Zero-Emission Vehicle (ZEV).

2.2Physical Description of a PEMFC

There are different technologies of fuel cell. They are commonly classified according to temperature or the type of electrolyte. Among others, low-temperature fuel cell includes Proton Exchange Membrane (PEM). Proton exchange membrane fuel cells (PEMFC) are promising new power sources for vehicle and portable devices. The schematic of Fuel Cells can be elucidated as two electrodes (anode and cathode) isolated by a solid membrane acting as an electrolyte as shown in Fig.2.a [5, 13].

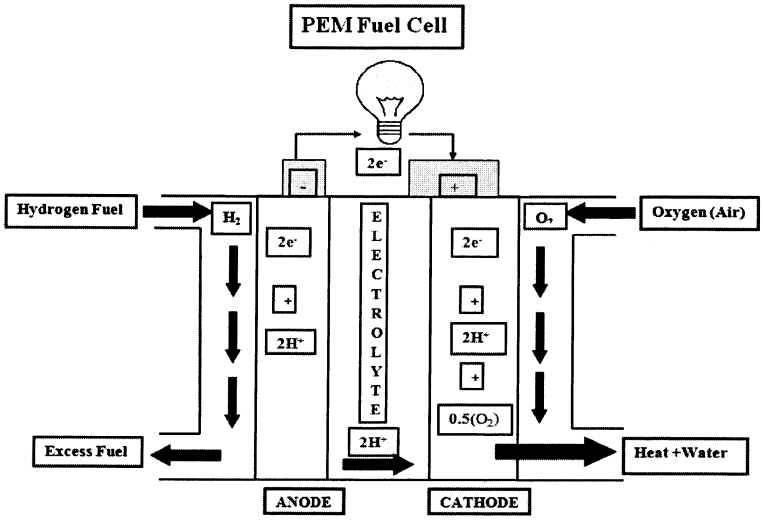

Fig. 2.a Schematic of a Fuel cell operation

The Hydrogen fuel flows into the anode, where it segregates into protons, which in turn, flows through the electrolyte to the cathode and hence the electrons are accumulated as electrical current by an external circuit linking the two electrodes. Similarly the oxygen flows into the cathode, where the oxygen combines with electrons in the external circuit and the protons that flow through the membrane, thereby producing water.

The chemical reactions in PEMFC can be described by the following equations [1, 2]

$$\begin{cases} H_2 \rightarrow 2H^+ + 2e^+ \\ 2H^+ + \frac{1}{2}O_2 + 2e^- \rightarrow H_2O \\ H_2 + \frac{1}{2}O_2 \rightarrow H_2O \end{cases} \tag{2.2.1}$$

The necessary power to the load is provided by the electrons flowing from anode to the cathode. Electricity is delivered adequately, when a number of fuel cells are connected in series which make up a fuel cell stack. The performance of the PEM fuel cells increased, when its operating temperature is around 70-80° Celsius at a partial reactant pressure of 3-5atm.

2.3 Equivalent Circuit of PEMFC

The dynamic behavior of a PEM fuel cell stack can be represented by means of a simple first-order equivalent circuit [5], [7], and [16] such as the one depicted in Fig. 3. The ohmic voltage drop is represented through the resistor R_{ohm}, which expresses the internal resistance of the cell stack, i.e., the resistance due to non-ideal electrodes and conductive plates and to proton transfer through the membrane [5] and [9].The activation voltage

drop is represented through the parallel connection of a resistor, R_{act}, with a capacitor, C, that models the double layer of charge at the interfaces between the membrane and the electrodes.

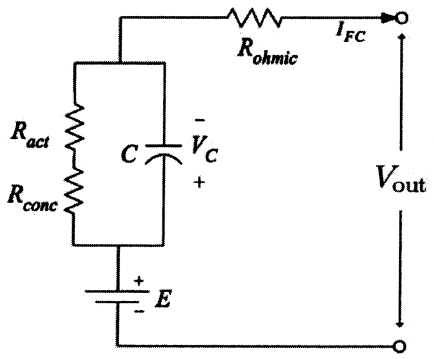

Fig:3 Equivalent Circuit of first order PEMFC

The Fig.3 does not give description of concentration voltage drop, related to changes in the concentration of oxygen and hydrogen at the electrodes, since it is not important for controlling the PEMFC current and voltage. Although in a well-designed system with good oxygen and hydrogen supplies this drop should be very small at the rated current [5], it may be taken into account by impedance in series with R_{act}. The elements of this simple circuit are assumed nonlinear. The simulation results in a linear steady-state performance curve that approximates the estimated performance curve just for intermediate current density values, but not for low or high current density values. The simulated results help us to present an equivalent circuit able to approximate both dynamic and steady-state behavior of the stack.

The two charged layers of opposite polarity are formed across the boundary between the porous cathode and the membrane [24,25], known as electrochemical double layer, can store electrical energy and behave like ultra capacitor.

2.4 Mathematical Modeling of PEMFC

The mathematical model is derived using Kirchhoff's current and voltage law from the equivalent circuit of PEMFC as shown in Fig.3. The output voltage across the fuel cell V_{out} can also be termed as the total voltage across the simple first order equivalent circuit of fuel cell(V_{fc}).The voltage across the fuel cell (V_{fc})is defined to be a function of the stack current, partial pressure of the reactants, temperature of the fuel cell and the humidity of the membrane.

$$V_{fc} = E_0 - V_{act} - V_{ohm} - V_{conc}$$
$$V_{tfc} = n(E_0 - V_{act} - V_{ohm} - V_{conc}) \qquad (2.4.1)$$

where n the number of the fuel cells in the stack, V_{tfc} is the total voltage across the fuel cell stack, E_0 is the thermodynamic cell potential or open circuit voltage, V_{act} .is the activation overvoltage across R_{act}, V_{ohm} is the ohmic voltage drop across the resistance R_{ohmic}, and V_{conc} is the mass transport voltage drop or the concentration across R_{conc}.

Thermodynamic cell potential

The open circuit voltage E_0, also known as thermodynamic potential or reversible cell voltage [17], is calculated as follows,

$$E_0 = 1.229 - 0.85 \cdot 10^{-3}(T_{fc} - 298.15) + 4.3085 \cdot 10^{-5} T_{fc}[\ln(P_{H_2}) + \frac{1}{2}\ln(P_{O_2})] \qquad (2.4.2)$$

where P_{H_2} is a partial pressure of hydrogen inside the fuel cell, P_{O_2} is a partial pressure of oxygen inside the fuel cell, and T_{fc} is an operating temperature of the fuel cell stack. The temperature T_{fc} in the membrane and the partial pressure of the gases changes with the fuel cell current. The temperature increases with the increasing current, whereas the partial pressures of the gases decrease.

Activation Over- Potential

This loss is caused due to the slow transferring of charge at the surface of the electrodes. A part of the electrode potential is used for driving transfer of electrons in order to match the current demand. Hence the voltage at the fuel cell drops. Thus the dynamics of activation over potential are given by,

$$\frac{dV_{act}}{dt} = \frac{i_L}{C_{dl}} - \frac{V_{act}}{R_{act}C_{dl}} \qquad (2.4.3)$$

where C_{dl} is a double layer capacitance, and R_{act} is the equivalent resistor to activation. The double layer of charge (*dl*) is an important concept, in order to understand the dynamics of the fuel cell. Whenever two materials of opposite charge come in contact, there is an accumulation of the charge on the surface of the materials or a transfer of load takes place from one to another. The charge layer that is deposited on the interface of the electrode or electrolyte acts a storage of the electrical charges and in this way, it acts an electrical capacitor C_{dl} [15].

Ohmic Over Potential

The ohmic over potential V_{ohm} results from the resistance to the transfer of electrons in the electrolyte [11]; the contact resistance present at the fuel cell terminals and the resistance to the transfer of the electrons through the electrodes.

$$V_{ohm} = i_L R_{ohm} \tag{2.4.4}$$

R_{ohm} is the equivalent resistor to the ohmic over potential, and i_{fc} is the current through the fuel cell.

Concentration Over- potential

This loss is also known as Mass transport voltage drop. The concentration of hydrogen and oxygen are affected by the mass transport. The drop in concentration of the gases, in turn, affects the pressure of the gases[14]. The electrical current and the physical characteristics of the system are directly proportional to the pressures of the oxygen and hydrogen. Maximum current density is defined, in order to determine the voltage drop, under which the fuel is being used at the same rate of the maximum speed.

Thus, the drop in voltage is caused due to the mass transport is calculated as follows,

$$V_{conc} = a\exp\left(bi_{fc}\right) \tag{2.4.5}$$

The coefficients vary with the temperature, where the values of the coefficients are given to be $a = (1.1*10^{-4} - 1.2*10^{-6}.(T_{fc} - 273))(V)$ and $b = 8*10^{-3}(cm^2 mA^{-1})$.s

2.5 Summary

This chapter mainly encloses the general overview of the fuel cell technology, elaborates the physical description of PEMFC and also elucidates the mathematical modeling of the PEMFC in detail.

Chapter 3

ELECTRICAL AND STATE SPACE MODELING OFDC-DC CONVERTERS

3.1 Introduction to DC-DC Converters

DC-DC power converters are mainly used to transform the electrical energy produced by the PEMFC to a much higher electrical power output. A DC-to-DC converter is a device that accepts a DC input voltage and produces an altered DC output voltage [24]. Typically the output produced is at a different voltage level than the input. In addition, DC-to-DC converters are used to provide noise isolation, power bus regulation, etc. In most of the applications, we want to change the DC energy from one voltage level to another, while wasting as little as possible in the process. In other words, we want to perform the conversion with the highest possible efficiency.

The aim of DC-DC power conversion is to obtain a regulated, continuous voltage at the load terminals. This is achieved through the use of power regulators [25].The power regulator consists of a power stage composed of semiconductors, inductors and capacitors, and a control stage commonly based on the processing of an error signal. The control objective is to achieve a regulated robust output voltage with good dynamic performance from the switching converter.

In this chapter, we will be studying the following,

- Derivation of electrical and state space models of the three basic types of DC-DC converter circuits namely, buck, boost and buck-boost

- Sliding mode control analysis and design strategies for DC-DC conversion problem.

3.2 Different types of DC-DC converters

There are three different types of DC-DC converters, each of which tends to be more suitable for certain type of applications. For better understanding of DC-DC converters, they can be studied and classified according to their applications [20]. The Buck converters are well-suited for stepping down the voltage. Hence, it can be used as step down converters in laptops or any other devices that requires less voltage. The Boost converters are only suitable for stepping up the voltage, thereby finding their applications in fuel cells and may others. The Buck-Boost converters are used for both stepping up and stepping down voltages.

3.2.1 DC-DC Buck Converter

The electrical and state space model of a buck converter is derived by feeding a resistive load as depicted in Fig.4.a. The buck converter dynamics are modeled by two state variables, i, inductor current and v, the capacitor voltage, and by the control input $u \in \{0,1\}$, which describes the position of a bidirectional switch [21]. The electrical modeling of the converter are listed below, where E is the DC-input voltage, L and C, the inductor and the capacitor values, respectively and R, the resistive load.

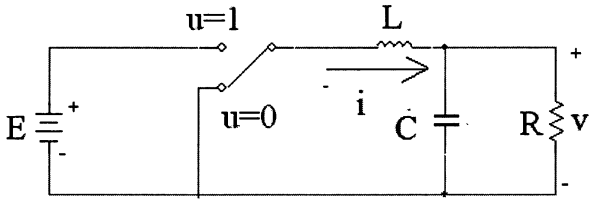

Fig.4.a. DC-DC Buck Converter

The dynamics of the buck converter are derived from the Fig.4.a .Thus the electrical model of buck converter is given as follows,

$$\begin{cases} L\dfrac{di}{dt} = -v + Eu \\ C\dfrac{dv}{dt} = i - \dfrac{v}{R} \end{cases} \tag{3.2.1.1}$$

A general model for buck converter is given in equation (10). Specific models can be obtained by selecting the parameters $\lambda = 0$ and $\gamma = 1$ as follows

$$\frac{d}{dt}\begin{pmatrix} Li \\ Cv \end{pmatrix} = \begin{pmatrix} 0 & -1+\lambda u \\ 1-\lambda u & \dfrac{-1}{R} \end{pmatrix}\begin{pmatrix} i \\ v \end{pmatrix} + \begin{pmatrix} E(1+\gamma(u-1)) \\ 0 \end{pmatrix} \tag{3.2.1.2}$$

When $\lambda = 0$ and $\gamma = 1$ is substituted in the equation (3.2.1.2)

$$\frac{d}{dt}\begin{pmatrix} Li \\ Cv \end{pmatrix} = \begin{pmatrix} 0 & -1 \\ 1 & \dfrac{-1}{R} \end{pmatrix}\begin{pmatrix} i \\ v \end{pmatrix} + \begin{pmatrix} E(1+(u-1)) \\ 0 \end{pmatrix} \tag{3.2.1.2.a}$$

Advantages of DC-DC Buck Converter

- Highly efficient
- Simplicity of design
- Minimal stress on the switch
- It requires a relatively small output filter for low output ripple.

Disadvantages of DC-DC Buck Converter

- There is no input to output isolation
- If the switch shorts, there is an overvoltage at the output

3.2.2 DC-DC Boost Converter

The electrical and state space model of a boost converter is derived by feeding a resistive load as depicted in Fig.4.b [25]. The boost converter dynamics are modeled by two state variables, i, inductor current and v, the capacitor voltage, and by the control input $u \in \{0,1\}$, which describes the position of a bidirectional switch. The dynamics of the converter are listed below, where E is the DC-input voltage, L and C, the inductor and the capacitor values, respectively and R, the resistive load [22].

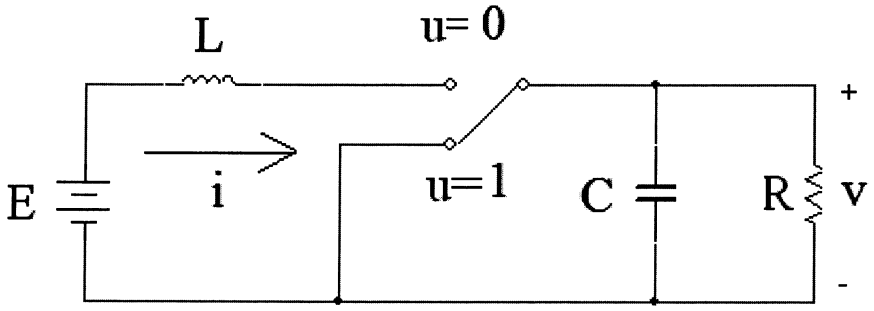

Fig.4.b. DC-DC Boost Converter

The dynamics of the boost converter are derived from the Fig.4.b .Thus the electrical model of boost converter is given as follows,

$$\begin{cases} L\dfrac{di}{dt} = -v(1-u) + E \\ C\dfrac{dv}{dt} = i - \dfrac{v}{R} \end{cases} \qquad (3.2.2.1)$$

The DC-DC boost converter model can be obtained by selecting the parameters $\lambda = 1$ and $\gamma = 0$. Thereby substituting these parameters in the equation (3.2.1.2), we obtain the state equation of the boost converter as follows [23],

$$\frac{d}{dt}\begin{pmatrix} Li \\ Cv \end{pmatrix} = \begin{pmatrix} 0 & -1+u \\ 1-u & \frac{-1}{R} \end{pmatrix}\begin{pmatrix} i \\ v \end{pmatrix} + \begin{pmatrix} E \\ 0 \end{pmatrix} \qquad (3.2.2.2)$$

Advantages of DC-DC Boost Converter

- Used in Hybrid Cars for their increased voltage mechanism
- The output voltage is greater than the input voltage
- Better power factor is achieved

Disadvantages of DC-DC Boost Converter

- The opening and closing of the switch must be faster for better efficiency
- The internal dynamics of the system [5.1.1] are unstable that causes problem while directly controlling the output voltage

3.2.3 DC-DC Buck-Boost Converters

The electrical and state space model of a buck-boost converter is derived by feeding a resistive load as depicted in Fig.4.c. The buck-boost converter dynamics are modeled by two state variables, i, inductor current and v, the capacitor voltage, and by the control input $u \in \{0,1\}$, which describes the position of a bidirectional switch [25]. There exists an output voltage polarity inversion with respect to the input voltage. The dynamics of the converter are listed below, where E is the DC-input voltage, L and C, the inductor and the capacitor values, respectively and R, the resistive load.

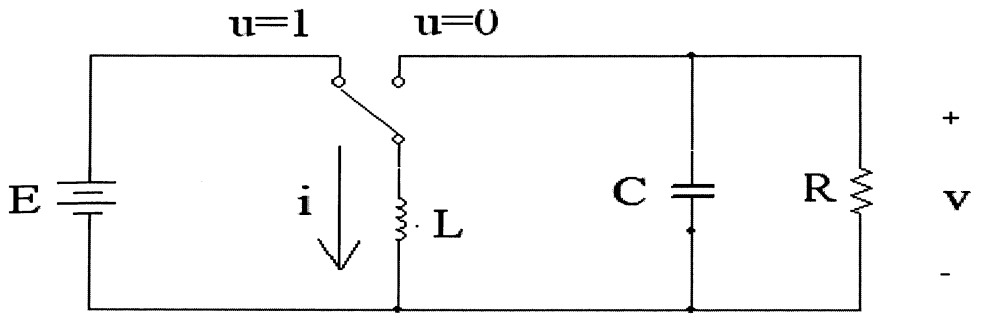

Fig.4.c. DC-DC Buck-Boost Converter

The dynamics of the buck-boost converter are derived from the Fig.4.c .Thus the electrical model of buck-boost converter is given as follows,

$$\begin{cases} L\dfrac{di}{dt} = -(1-u)v + Eu \\ C\dfrac{dv}{dt} = (1-u)i - \dfrac{v}{R} \end{cases}$$

(3.2.3.1)

The DC-DC boost converter model can be obtained by selecting the parameters $\lambda = 1$ and $\gamma = 1$.Thereby substituting these parameters in the equation (8), we obtain the state equation of the boost converter as follows,

$$\frac{d}{dt}\begin{pmatrix} Li \\ Cv \end{pmatrix} = \begin{pmatrix} 0 & -1+u \\ 1-u & \dfrac{-1}{R} \end{pmatrix}\begin{pmatrix} i \\ v \end{pmatrix} + \begin{pmatrix} E(1+(u-1)) \\ 0 \end{pmatrix} \qquad (3.2.3.2)$$

Advantages of DC-DC Buck-Boost Converter

- They produce an output voltage much larger than the input voltage
- They can produce a wide range of output voltage from that maximum output voltage to almost zero
- The output voltage is adjustable based on the duty cycle of the switching transistor

Disadvantages of DC-DC Buck-Boost Converter

- The switch does not have a terminal at ground, this complicates the driving circuitry
- If the power supply is isolated from the load circuit, the diode polarity can simply be reversed.
- Unstable internal dynamics

3.3 Sliding mode control analysis and design

Chapter 5, elucidates the basic introduction and necessity of Sliding Mode Control (SMC). It is essential to study the SMC strategies for better understanding of conversion challenges faced by the DC-DC converters. Output voltage regulation is the general control objective in DC-DC power conversion [20]. A naïve approach would design the action of the switch, the control action, based uniquely on the output voltage error (direct control). This approach will not be successful in general. An indirect approach, based on both the output voltage and the inductor current, is needed to achieve robust regulation.

Sliding mode control strategies for the DC-DC conversion problem via direct and indirect control will be considered here [21]. Starting from a switching surface, the transversality condition is checked and the equivalent control is derived [25]. The latter is used to obtain the ideal sliding dynamics are stable, to deduce the sliding domain.

3.3.1Direct output voltage control

First, let us consider a direct output voltage control, which implies the use of the switching surface [22],

$$\sigma_v = v - V_{ref} \tag{3.3.1.1}$$

Where $V_{ref} > 0$ is a constant output voltage reference. Note that the transversality condition is not fulfilled in the buck converter case ($\lambda = 0$).

For other cases,($\lambda = 1$ and $i \neq 0$), the equivalent control and the ideal sliding dynamics are given by [23]

$$u_{eq} = \frac{i - (V_{ref} / RC)}{i} \tag{3.3.1.2}$$

$$\begin{cases} v = V_{ref} \\ \dfrac{di}{dt} = \dfrac{1}{Li}\left(Ei - \dfrac{V_{ref}}{R}(E\gamma + V_{ref}) \right) \end{cases} \tag{3.3.1.3}$$

The ideal sliding dynamics has an equilibrium point at($(E\gamma + V_{ref})V_{ref} / RE, V_{ref}$).Its stability is analyzed by the first linear approximation, namely

$$\frac{d\hat{i}}{dt} = \frac{R}{L}\frac{E^2}{V_{ref}(E\gamma + V_{ref})}\hat{i} \tag{3.3.1.4}$$

Where $\hat{i} = i - i^*$ and $i^* = (E\gamma + V_{ref})V_{ref} / RE$. Since (R/L) $(E^2 / V_{ref}(E\gamma + V_{ref})) > 0$, the equilibrium point is unstable; hence direct voltage regulation results in instability of the inductor current.

3.3.2 Indirect output voltage control

Now the proposed switching surface is [23],

$$\sigma_i = i - i_{ref} \tag{3.3.2.1}$$

where i_{ref} denotes a constant inductor current reference. Then, the equivalent control and the ideal sliding dynamics are given by [25],

$$u_{eq} = \frac{v - E(1-\gamma)}{E\gamma + \lambda v} \tag{3.3.2.2}$$

$$\begin{cases} i = I_{ref}, \\ \dfrac{dv}{dt} = \dfrac{1}{C}\left(I_{ref} - \lambda I_{ref}\left(\dfrac{v - E(1-\gamma)}{E\gamma + \lambda v} \right) - \dfrac{v}{R} \right) \end{cases} \tag{3.3.2.3}$$

The geometric locus defined by the equilibrium points is described in coordinates (I_{ref}, v^*) by $v^{*2} + E\gamma v^* - EI_{ref}R = 0$ for $\lambda = 1$ and $v^* = I_{ref}R$ for $\lambda = 0$. Linearizing (18) around the equilibrium point (I_{ref}, v^*) yields

$$\frac{d\hat{v}}{dt} = \frac{1}{C}\left(-I_{ref}E\left(\frac{\lambda}{E\gamma + \lambda v^*} \right)^2 - \frac{1}{R} \right)\hat{v} \tag{3.3.2.4}$$

where $\hat{v} = v - v^*$.

Thus the indirect control results in a stable ideal sliding dynamics. The sliding domain on $i = I_{ref}$ resulting from $0 < u_{eq} < 1$, assuming E>0, gives the following converter characteristics.

Types of DC-DC converters	Characteristics	Sliding domain
Buck	Step-down	$i = I_{ref}$ and $0 < v < E$
Boost	Step-up	$i = I_{ref}$ and $0 < E < v$
Buck-Boost	Step-up/Step-down	$i = I_{ref}$ and $0 < v$

Finally, the switching strategy is defined so that $\frac{1}{2}\sigma_i^2$ qualifies as a Lyapunov function and its derivative is enforced to be negative by SMC 'u' [23].

$$\frac{1}{2}\frac{d\sigma_i^2}{dt} = \sigma_i \frac{d\sigma_i}{dt} = \sigma_i(\lambda v + E\gamma) - (u - u_{eq}) \qquad (3.3.2.5)$$

Then, since $0 < u_{eq} < 1$ is assumed,

$$u = \begin{cases} u = 0 & if\ \sigma_i(\lambda v + E\gamma) > 0 \\ u = 1 & if\ \sigma_i(\lambda v + E\gamma) < 0 \end{cases}$$

In summary, the indirect output voltage control provides output voltage regulation presuming the converter states meet the sliding domain conditions. However, the output voltage depends on the load resistance. Therefore, these controllers do not produce systems that are robust with respect to load variations.

3.4 Coupling of Boost converter with Fuel Cell

Though we studied various DC-DC power converters in the previous sections of this chapter, the boost converter is well suited as a power converter in case of Fuel cells. The main purpose of implementing a DC-DC boost converter is to increase the voltage produced by the fuel cell. In this section, we build the first stage of the Fuel cell system by coupling the equivalent circuit of PEMFC with the boost converter. The Fig.5.a explains the coupling of the equivalent circuit of PEMFC with the Boost converter.

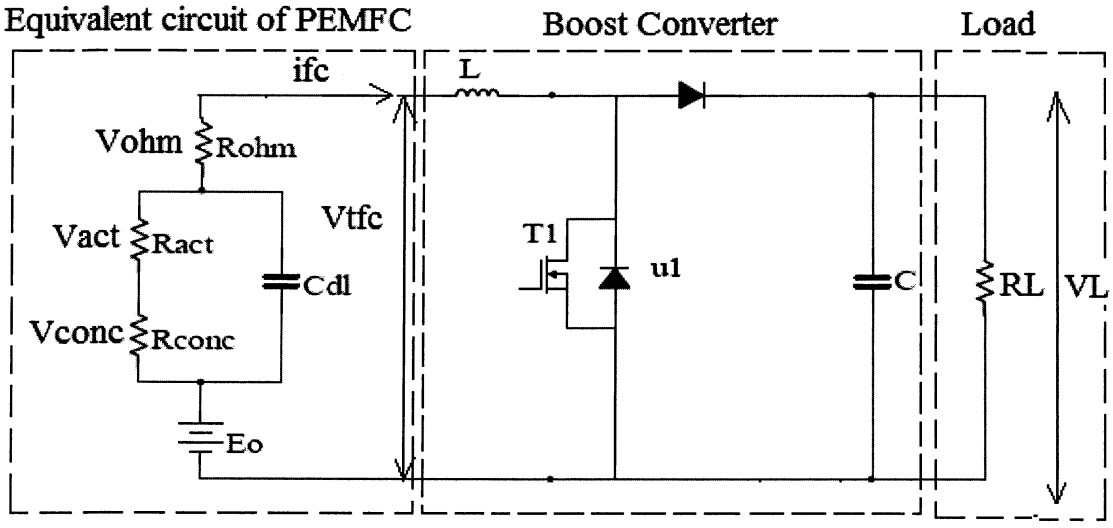

Fig.5.a. Coupling of equivalent circuit of PEMFC with the Boost converter

The dynamics of the boost DC-DC power converter are well-studied, see for instance [3, 4], and are governed by the following system of bilinear differential equations.

$$\frac{di_L}{dt} = -(1-u_1)\frac{1}{L}V_L + \frac{V_{ifc}}{L}$$
$$\frac{dV_L}{dt} = (1-u_1)\frac{1}{C}i_L - \frac{V_L}{R_L}\frac{1}{C} \qquad (3.4.1)$$

where $u_1 \in [0,1]$ is a switch control function. *Vtfc* is the total voltage produced across the fuel cell. V_L is the output voltage delivered to the load resistor R_L .In particular, $u_1 = 1$ when the switch is closed and $u_1 = 0$ when it is opened. In order to achieve the control symmetry, the control function is transformed as

$$u_1 = v_1 + 0.5 \tag{3.4.2}$$

Therefore, a new control function $v_1 \in [-0.5, 0.5]$ will replace u_1 in equation (3.4.1).

3.5 Summary:

In this chapter, the ideal buck, boost and buck-boost topologies are studied by feeding a resistive load and their respective electrical and state space models are derived accordingly. Sliding mode control strategies are discussed and designed to overcome challenges faced by the DC-DC power converters. The first stage of the thesis is completed by coupling the equivalent circuit of PEMFC with the boost converter.

Chapter 4

ULTRACAPACITORS

4.1 Basics of Ultra capacitors

An Ultra capacitor is a type of capacitor. A capacitor is an electronic unit that releases an electric charge to power devices. An Ultra capacitor is a capacitor with remarkably high power and energy density, giving them much higher efficiency. Ultra capacitors can also be described as mechanical batteries, due to their similarities to chemical batteries, and are very small in size. These Ultra capacitors have stepped up to the forefront of the capacitor field because of their high capacitance and their multiple advantages over traditional capacitors and batteries. Ultra capacitor was first generally used as low power, low energy, and long-life back-up power sources for consumer electronics.

4.2 Working of Ultra capacitors

An Ultra capacitor has two plates that are separated by a dielectric. The plates are made from a porous substance such as powdery, activated charcoal, which effectively gives them a larger area for storing charge.

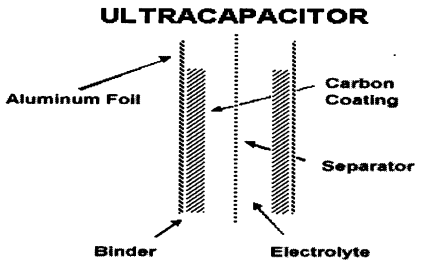

Fig.6.Schematic of an ultra capacitor

The Ultra capacitor has an electrolyte within it, separating the plates. In a conventional capacitor, positive charges form on one side and negative charges on the other with the dielectric placed in between them, keeping the charges safely apart. In an Ultra capacitor, the electrolyte is electrically active and adds another dimension, that is, the charged plates polarize the electrolyte, making positive ions inside it and negative ions on the other. Thereby causing a second set of charges to form, called a double-layer that allows the plates to store charge. Unlike in a battery, the positive and negative charges in an Ultra capacitor are produced entirely by static electricity, no chemical reactions are involved.

4.3Ultracapacitors Versus Batteries

Ultra capacitors function by supplying large bursts of energy to power a product and then quickly recharging themselves. Their extraordinarily low internal resistance, or "Equivalent Series Resistance (ESR)", permits them to deliver and absorb these high energy currents, whereas the higher internal resistance of a traditional chemical battery would cause the battery voltage to collapse. The Fig.6.a elaborates the comparative study of ultra capacitors and batteries.

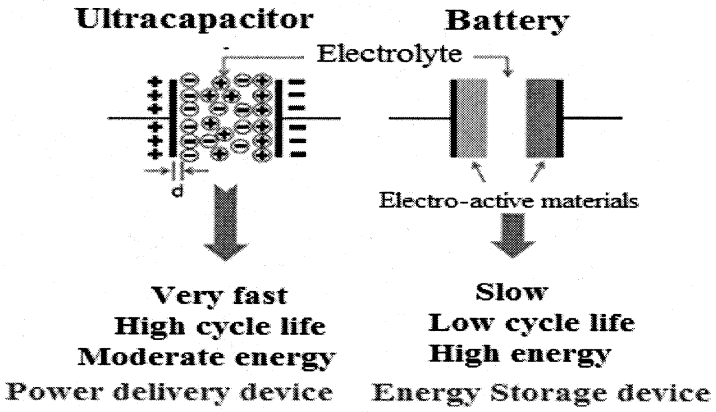

Fig.6.a Comparative study of working models of Ultra capacitors and Batteries

The mechanical charge carrier mechanisms of the Ultra capacitor give them an advantage over the chemical batteries. Also, while a battery generally demands a long recharging period, Ultra capacitors can recharge very quickly, usually within a matter of minutes. They also retain their ability to hold a charge, even after multiple recharging. When combined with a battery, an Ultra capacitor can remove the instantaneous energy demands that would normally be placed on the battery, lengthening the battery's running time and slowing down the battery's loss of charging capacity over time.

Batteries often require maintenance and can only operate well within a small temperature range. Ultra capacitors are maintenance free and perform well over a broad temperature range. They have an additional advantage over batteries with their Proton Exchange, an ultra capacitor fuel-cell technology. The hybridization of ultra capacitor - fuel cell leads to a high-efficiency energy conversion device, which is designed to operate perpetually as long as there is hydrogen fuel available to it. Ultra capacitor PEMs are environmentally friendly and thereby making ultra capacitors a highly reliable source of

backup power for applications (Fig.6.a). Although batteries are also capable of providing backup power, ultra capacitors have a distinct advantage over them as a backup power source because of the limited energy needs of backup power sources and the crucial need for backup power source reliability.

4.4 Mathematical Modeling of Ultra capacitors

The primary energy is stored by recovering the break energy using the ultra capacitor. The mechanism used in these capacitors for storage of energy is highly reversible. This reversible mechanism enables the ultra-capacitor to charge and discharge several times. The fuel starvation in the system is completely avoided by delivering high band frequency spectrum load power.

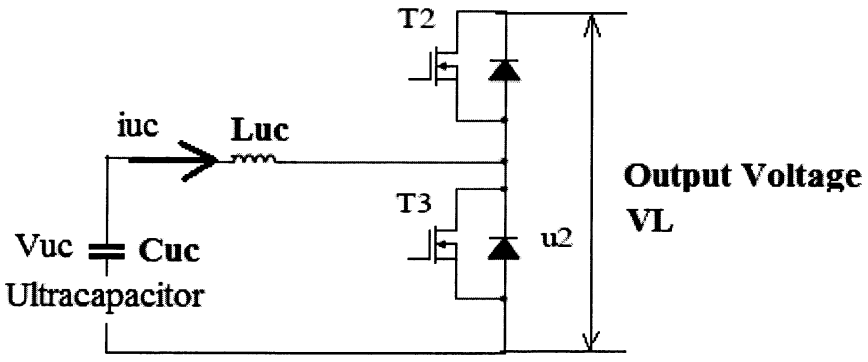

Fig.6.b Ultra capacitor coupled with Transistors

The ultra capacitor is built with transistors T2 and T3 initially as shown in Fig.6.b. Later this model (Fig.6.b) is coupled with the (Fig.5.a) to complete the second stage of the thesis. The entire fuel cell system is designed in this section. The design of the fuel cell

system encloses the equivalent circuit of the PEMFC, boost converter and the ultra capacitor. The mathematical model of the ultra capacitor is derived from the Fig.6.c. In Fig.6.c, under charging mode (as a buck converter), T2 acts as a switch and T3 acts as a diode, thereby serving as a unidirectional buck converter that collects the dc bus energy to charge the ultra capacitor. In discharging mode (as a boost converter), T3 acts a switch and T2 acts as a diode, thereby delivering the energy from the ultra capacitor back in to the DC bus. The complete dynamics of the ultra capacitors are derived by combining the Fig.6.b with the Fig5.a,

$$\frac{di_{uc}}{dt} = \frac{1}{L_{uc}}\left[-(1-u_2)V_L + V_{uc}\right]$$
$$\frac{dV_{uc}}{dt} = -\frac{1}{C_{uc}} i_{uc} \qquad (4.4.1)$$

where $u_2 \in [0,1]$ is a switch control function. V_{uc} , i_{uc} is the respective voltage and current across the ultra capacitor. In particular, $u_2 = 1$ when the switch is closed and $u_2 = 0$ when it is opened. In order to achieve the control symmetry, the control function is transformed as

$$u_2 = v_2 + 0.5 \qquad (4.4.2)$$

Therefore, a new control function $v_2 \in [-0.5, 0.5]$ will replace u_2 in eqs (4.4.1) and (4.4.2).

4.5 Summary

In chapter, we study in detail about the ultra capacitors. The working of the ultra capacitors is briefly summarized and a comparative study is done between the batteries and the ultra capacitors in order to bring about the vitality of the ultra capacitors as an energy management device. The second stage of thesis is completed by deriving the mathematical model of the ultra capacitor. The mathematical model of the ultra capacitor enables us to build the entire system dynamics in the next chapter.

Chapter 5

MATHEMATICAL MODELING AND CONTROL PROBLEM FORMULATION OF THE FUEL CELL SYSTEM

5.1 Mathematical Modeling of Fuel Cell System

The mathematical model of the fuel cell system dynamics is derived by combining the mathematical models of PEMFC, boost DC-DC power converter and the ultra capacitor. A stack of n considered PEMFC'S are used, altogether with the ultra capacitor, as a primary source of electrical energy for the boost DC-DC power converter. In order to derive the dynamics of the ultra capacitor, equivalent circuit of the fuel cell system was derived in the chapter 4. The equivalent circuit of a single stack of PEMFC combined with the power converter and a power converter is shown in the Fig.7

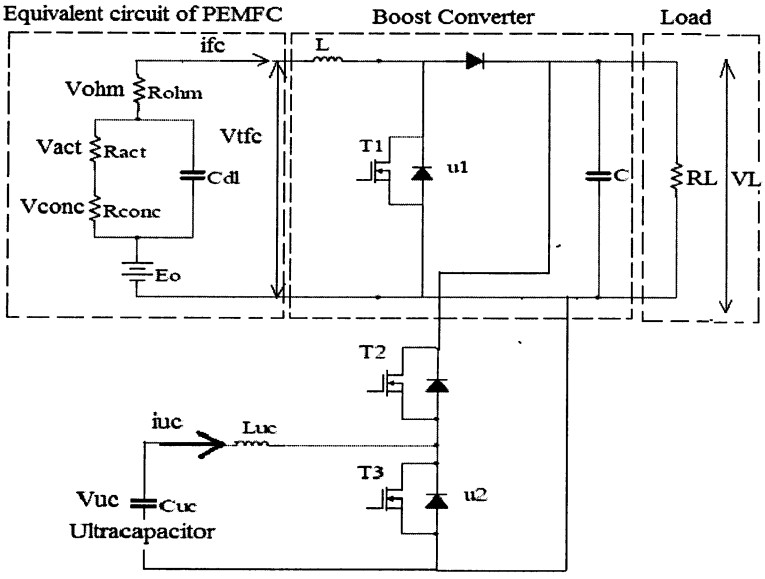

Fig.7 Equivalent circuit of a single stack of PEMFC of the Fuel cell system

ifc is the Fuel cell current same as the current through the inductance i_L. R_L is the resistance of the load. v_{cf}, is the voltage across the capacitor C_{dl}. V_{tfc} , is the total voltage across the PEMFC equivalent circuit. V_L,is the output voltage across the load. R_{var} , is the variable internal resistor of the fuel cell.

Combining the equations from the chapter 2 (2.4.1-2.4.5) , chapter 3 (3.4.1-3.4.2) and chapter 4(4.4.1-4.4.2) we derive the mathematical model of the fuel cell system,

$$\begin{cases} \dfrac{di_L}{dt} = -\dfrac{1}{L}[\dfrac{1}{2}V_L - n(1.229 - 0.85\cdot 10^{-3}(T_{fc} - 298.15) + \\ \qquad 4.3085\cdot 10^{-5}T_{fc}(\ln(P_{H_2}) + \dfrac{1}{2}\ln(P_{O_2})) - \\ \qquad V_{act} - i_L R_{ohm} - m\exp(ji_{fc}))] + \dfrac{V_L}{L}v_1 \\ \dfrac{dV_L}{dt} = \dfrac{1}{C}\left(\dfrac{1}{2}i_L - \dfrac{V_L}{R_L}\right) - \dfrac{1}{C}i_L v_1 \\ \dfrac{dV_{act}}{dt} = \dfrac{i_L}{C_{dl}} - \dfrac{V_{act}}{R_{act}C_{dl}} \\ \dfrac{di_{uc}}{dt} = \dfrac{1}{L_{uc}}[-(0.5 - v_2)V_L + V_{uc}] \\ \dfrac{dV_{uc}}{dt} = -\dfrac{1}{C_{uc}}i_{uc} \end{cases} \tag{5.1.1}$$

5.2 Control Problem Formulation

The goal of this paper is to design the sliding mode controller in terms of controls P_{O_2}, v_1, v_2 that make the output voltage V_L of the boost DC-DC converter to follow a given reference profile $V_{Lc}(t)$ in the presence of unknown bounded parameters of PMEFC R_{conc}, C_{dl}, R_{ohm} and the load resistor R_L. The ultra capacitor is supposed to be controlled

in two possible regimes: V_{uc} charging mode (when the ultra capacitor takes charge from the fuel cell) and i_{uc} control mode (when the ultra capacitor provides "fast" portion of the load current to the load).

In fact, direct control of the output voltage in the boost DC-DC power converters is a non-minimum phase problem [13] that adds complexity to the controller design [3, 4].In the case of system (5.1.1) there exists a possibility to control the PEMFC current i_{fc} that is equal to the inductance current i_L using the control function P_{O_2}. Therefore, in addition to controlling the output voltage we will drive the inductance current i_L to follow a "slow" portion of the command profile $i_{Lc}(t)$.

Thus the given system (5.1.1) can be divided into three subsystems for better formulation of the control problem. Relative degree approach enables us to formulate the control problem.

Control Problem Formulation of DC-DC Boost converter

Using the relative degree approach [13], the *input-output* dynamics of boost DC-DC power converter of *relative degree 1* are presented in a de-coupled format as

$$\frac{dV_L}{dt} = \varphi_2(i_L, V_{L,} R_L) - \frac{1}{C} i_L v_1$$

(5.1.3)

$$\varphi_2(i_L, V_{L,} R_L) = \frac{1}{C}\left(\frac{1}{2} i_L - \frac{V_L}{R_L}\right), \qquad (5.1.4)$$

Control Problem Formulation of PEMFC

The output current and voltage is given to be i_L and V_L. P_{H_2} is the pressure of hydrogen. The input dynamics of PEMFC mainly depends on pressure of hydrogen, activation overvoltage (2.4.3) and the output current and voltage.

$$\frac{di_L}{dt} = \varphi_1(i_L, V_L, V_{act}, P_{H_2}) + \omega_1 \tag{5.1.5}$$

Where,

$$\varphi_1(i_L, V_L, V_{act}, P_{H_2}) = -\frac{1}{L}[\frac{1}{2}V_L - n(1.229 - 0.85\cdot 10^{-3}(T_{fc} - 298.15) + 4.3085\cdot 10^{-5} T_{fc} \ln(P_{H_2}) \\ -V_{act} - i_L R_{ohm} - a\exp(bi_{fc}))] \tag{5.1.6}$$

$$\omega_1 = \frac{1}{L}\left[V_L v_1 + 2.15425\cdot 10^{-5} T_{fc} n \ln(P_{O_2})\right]. \tag{5.1.7}$$

The control problem is to design continuous control function ω_1 that drives i_L to i_{Lc} as time increases in the presence of uncertain parameters R_L and R_{ohm}. This generates i_{Lc} based on the power balance. The generated power is to be equal to consumed power. The actual PEMFC control function is given in terms of P_{O_2} and can be easily calculated from the equation(5.1.7)as soon as ω_1 is generated.

Control Problem formulation of Ultra capacitor

The *input-output* dynamics of the ultra capacitor of *relative degree 2* are derived for the charge mode in an ultra capacitor is derives as follows,

$$\frac{d^2V_{uc}}{dt^2} = \varphi_3(V_L, V_{uc}) - \frac{V_L}{C_{uc}L_{uc}}v_2 \tag{5.1.8}$$

The *input-output* dynamics of the ultra capacitor of *relative degree 1* are derived for the current control mode

$$\frac{di_{uc}}{dt} = -C_{uc}\left(\varphi_3(V_L, V_{uc}) - \frac{V_L}{C_{uc}L_{uc}}v_2\right) \tag{5.1.9}$$

where

$$\varphi_3(V_L, V_{uc}) = -\frac{1}{C_{uc}L_{uc}}\left(-0.5V_L + V_{uc}\right) \tag{5.1.10}$$

The outputs (5.1.2) can be easily controlled using the input-output dynamics (5.1.3)-(5.1.9) by the control inputs ω_1, v_1, v_2 designed in the formats of classical SMC and HOSM control with gain adaptation in the presence of the bounded disturbances/uncertainties $\varphi_1, \varphi_2, \varphi_3$, assuming the PEMFC current i_L is bounded. The derivative of the disturbance φ_1 is assumed to be bounded, i.e. $|\dot{\varphi}_1| \le M_1$ with the unknown boundary M_1, and the disturbances φ_2, φ_3 are also assumed to be bounded, i.e. $|\varphi_2(i_L, V_L, R_L)| \le M_2$.

Now, **the problem can formulated** as designing the control functions $\omega_1, \omega_2, \omega_3$ so that $e_1, e_2, e_3 \to 0$ in finite time,

where $e_1 = y_{1c} - y_1$, $e_2 = y_{2c} - y_2$, and $e_3 = y_{3,1_c} - y_{3,1}$ in the "fast" load current control mode or $e_3 = y_{3,2_c} - y_{3,2}$ in the ultra capacitor charge mode; here $y_{1c}, y_{2c}, y_{3,1_c}, y_{3,2_c}$ are command

profiles. Denoting the controlled and measured outputs as $y_1 = i_L$, $y_2 = V_L$, $y_{3,1} = i_{uc}$, $y_{3,2} = V_{uc}$. It is assumed that the hydrogen pressure P_{H_2} is stabilized on a required level by means of a hydrogen pump. The P_{H_2} stabilization problem is out of scope of this work. Assuming that the current i_L has been driven to its reference profile $i_{Lc}^{slow}(t)$ by control ω_1, the respective forced *zero* dynamics [13] become apparently stable.

$$\frac{dV_{act}}{dt} + \frac{V_{act}}{C_{dl}R_{act}} = -\frac{1}{C_{dl}} i_{Lc}^{slow}(t) \tag{5.1.11}$$

Also, in the case of controlling the current i_{uc}, and assuming $i_{uc} = i_{Load}^{fast}$ the associated stable forced zero dynamics are

$$\frac{dV_{uc}}{dt} = -\frac{1}{C_{uc}} i_{Load}^{fast} \tag{5.1.12}$$

The stability of zero dynamics (5.1.11) and (5.1.12) makes systems (5.1.1) and (5.1.3)-(5.1.9) of a minimum phase that simplifies the controller design.

5.3 Summary:

The mathematical model of the fuel cell system is derived by combining dynamics of the PEMFC, DC/DC boost converter and ultra capacitor from their respective chapters 2, 3 and 4. The control problem formulation of the entire system is formulated based on the relative degree approach that is used for deriving the input-output dynamics of the various components present in the system.

Chapter 6

SMC CONTROLLER DESIGN FOR SYSTEM OF ELECTRIC POWER SUPPLY: PEMFC/DC-DC CONVERTER/ULTRACAPACITOR

This chapter is the backbone of the entire thesis, since it elaborates the controller design for the Fuel cell System. Relative degree approach is applied for direct control of the output load voltage, the fuel cell and ultra capacitor current/voltage in the presence of the model uncertainties. Adaptive second order super-twisting control, in terms of the oxygen pressure, is used to control the PEMFC current. Traditional sliding mode controllers control the DC-DC boost power converter and the ultra capacitor in a charge/discharge mode.

6.1 Inductance current controlled using adaptive-gain 2-SMC controller design

The inductance current controller is supposed to be continuous, while driving $e_1 \to 0$ in finite time in accordance with equation (5.1.5). The adaptive-gain 2-SMC super-twisting algorithms drives the output tracking errors to zero in finite time in the presence of bounded disturbances which bounds are unknown. The other advantage is in achieving non-overestimated control gains that reduce chattering.

Consider the system discussed in chapter 5. Recalling the equation (5.1.1), We divide the system of equations into three major subsystems. We initially consider the PEMFC subsystem and derive the tracking error dynamics of the inductance/PEMFC .

$$\frac{di_L}{dt} = \varphi_1(i_L, V_L, V_{act}, P_{H_2}) + \omega_1 \tag{6.1.1}$$

In accordance with Theorem 1 the ASTW control is designed in a form

$$\begin{aligned}
&\omega_1 = \alpha|e_1|sign(e_1) + \omega_{1,2}, \quad \dot{\omega}_{1,2} = \frac{\beta}{2}sign(e_1) \\
&\dot{\alpha} = \begin{cases} \frac{\varpi}{\sqrt{2}}sign(|e_1| - \mu), & if \ \alpha > \alpha_m \\ \eta, & if \ \alpha \le \alpha_m \end{cases} \\
&\beta = 2\varepsilon\alpha, \quad \alpha(0) > \alpha_m
\end{aligned} \tag{6.1.2}$$

The equation (5.1.7)is solved to be,

$$\begin{aligned}
&P_{O_2} = \begin{cases} \exp\left(\frac{L\omega_1 + 0.5V_L sign(e_2)}{2.15425 \cdot 10^{-5} T_{fc} n}\right), & if \ t \le t_r \\ \exp\left(\frac{L\omega_1 - V_L v_{1eq}}{2.15425 \cdot 10^{-5} T_{fc} n}\right), & if \ t > t_r \end{cases} \\
&u_1 = 0.5(1 - sign(e_2)) \\
&u_2 = \begin{cases} 0.5(1 - sign(\sigma_1)), & \text{in the voltage charge mode} \\ 0.5(1 - sign(\sigma_2)), & \text{in the current control mode} \end{cases}
\end{aligned} \tag{6.1.3}$$

Where

ω_1 is the ASTW control law given by equations (6.1.2),

t_r is a finite reaching time in the load voltage control loop, and v_{1eq} is equivalent control of v_1 that can be identified via v_1 low pass filtering, for instance, as

$$\tau_2 \dot{v}_{1eq} + v_{1eq} = v_1, \quad \tau_2 > 0 \tag{6.1.4}$$

$$e_1 = y_{1c} - y_1 \tag{6.1.5}$$

$$y_1 = i_L, y_{1c} = i_{Lc}\ e_1 = i_L - i_{Lc} \tag{6.1.6}$$

Remark:

The complexity of equation (6.1.3) is caused by the necessity to obtain **continuous** control P_{O_2}

6.1.2. The Inductance current command generator

The inductance current command is computed based on the power balance $P_{\text{PMEFC}} = P_{Load}$. The power balance will be fulfilled if the inductance current command is generated as

$$i_{Lc} = i^c_{Load}\frac{y_{2c}}{V_{tfc}}, \qquad i^c_{Load} = \frac{y_{2c}}{R_L} \tag{6.1.7}$$

where i^c_{Load} is the load current command, V_{tfc} is assumed to be measured, $y_{2c} = V_{Lc}$, and the load resistance R_L is to be identified. This command is split in two parts

$$i_{Lc} = i^{slow}_{Lc} + i^{fast}_{Lc} \tag{6.1.8}$$

where i_{Lc} is supposed to follow i^{slow}_{Lc} profile. while i_{uc} will follow the command profile i^c_{uc} that is the fast part of the load current command profile i^{fast}_{Load}.

The command profiles $i^{slow}_{Lc}, i^{fast}_{Load} = i^c_{uc}$ can be generated as

$$\tau \frac{di_{Lc}^{slow}}{dt} = -i_{Lc}^{slow} + i_{Load}^{c}$$
$$i_{Load}^{fast} = \frac{V_{tfc}}{y_{2c}}\left(i_{Load}^{c} - i_{Lc}^{slow}\right) \tag{6.1.9}$$

This power management is due to the fact that the compensated dynamics of the oxygen pump is relatively slow with respect the dynamics of the ultra capacitor. The load resistance R_L is to be identified on line, in order to generate the current commands in equations. (6.1.7, 6.1.9)

6.2 Sliding Mode Controller Design for the Output voltage of the Boost DC-DC Converter

The dynamics of the output voltage tracking error are derived

$$\dot{e}_2 = \underbrace{\dot{y}_{2c} - \varphi_2(i_L, V_{L,} R_L)}_{\psi(i_L, V_{L,} R_L)} + \frac{1}{C} i_L v_1 \tag{6.1.10}$$

Where the combined disturbance $\psi(i_L, V_{L,} R_L)$ is assumed bounded, i.e. $\left|\psi(i_L, V_{L,} R_L)\right| \le \bar{M}_2$. The output voltage controller is supposed to be discontinuous, since it represents a switching function $v_1 \in [-0.5, 0.5]$. The viable candidate for this controller is a traditional sliding mode controller (SMC)

$$v_1 = -0.5 sign(e_2) \tag{6.1.11}$$

The sliding mode existence condition [5]:

$$e_2 \dot{e}_2 \le -\rho |e_2|, \ \rho > 0 \tag{6.1.12}$$

where ρ is to be selected to provide for a given reaching time $t_r \le \frac{e_2(0)}{\rho}$, are to be verified for the controller (6.1.11). Substituting eq. (6.1.11) into eq. (6.1.12) we obtain

$$e_2\dot{e}_2 = e_2\left(\psi - \frac{i_L}{2C}sign(e_2)\right) \le |e_2|\left(\bar{M}_2 - \frac{i_L}{2C}\right) \le -\rho|e_2| \tag{6.1.13}$$

Given $C, \bar{M}_2$ and ρ, the existence condition (6.1.12) will be satisfied if

$$i_L \ge 2C(\bar{M}_2 + \rho) \tag{6.1.14}$$

It means the command to the inductance current i_{Lc} must be large enough in order to fulfill inequality (6.1.14).

6.3 Ultra capacitor Control

The output voltage and current from an ultra capacitor is controlled using the classical sliding mode control.

6.3.1The voltage charge control mode

In the voltage charge control mode the ultra capacitor dynamics given by (5.1.12) can be robustly controlled by classical SMC, since these dynamics are inherently fast, so that $V_{uc} \to V_{uc}^c$ as time increases:

$$\frac{d^2V_{uc}}{dt^2} = \varphi_3(V_{L,}V_{uc}) - \frac{V_L}{C_{uc}L_{uc}}v_2$$

$$\varphi_3(V_L, V_{uc}) = -\frac{1}{C_{uc}L_{uc}}(-0.5V_L + V_{uc}) \tag{6.1.15}$$

$$e_3 = y_{3,2_c} - y_{3,2}\ y_{3,2c} = V_{uc}{}^{c}\ \ y_{3,2} = V_{uc}$$

The following control function is derived based on SMC design algorithm presented in Chapter 6

$$v_2 = -0.5sign(\sigma_1)$$
$$\sigma_1 = \dot{e}_3 + \gamma e_3, \quad e_3 = V_{uc}^{c} - V_{uc}$$

6.3.2The current charge control mode

In the current control mode the ultra capacitor dynamics given by (5.1.13) is also controlled by classical SMC, so that $i_{uc} \to i_{uc}^{c}$ as time increases:

$$\frac{di_{uc}}{dt} = -C_{uc}\left(\varphi_3(V_{L,}V_{uc}) - \frac{V_L}{C_{uc}L_{uc}}v_2\right)$$

$$\varphi_3(V_L,V_{uc}) = -\frac{1}{C_{uc}L_{uc}}(-0.5V_L + V_{uc}) \qquad (6.1.16)$$

$$e_3 = y_{3,1_c} - y_{3,1}\ y_{3,1c} = i_{uc}{}^{c}\ \ y_{3,1} = i_{uc}$$

The following control function is derived based on SMC design algorithm presented in Chapter 6

$$v_2 = 0.5sign(\sigma_2)$$
$$\sigma_2 = e_4, \quad e_3 = i_{uc}^{c} - i_{uc}$$

The existence of the sliding modes in systems (5.1.12), (6.1.15) and (5.1.13), (6.1.16) can be easily assessed similar to Section 6.2

6.4 Identification of Load Resistance

The unknown load resistance R_L that is supposed to be used in computing the current command profiles in equations (6.1.8), (6.1.9) is identified via the sliding mode observer using equation. (3.4.1)

$$\frac{d\hat{V}_L}{dt} = \frac{1}{C}\left(\frac{1}{2}i_L - \frac{V_L}{R_{L0}}\right) - \frac{1}{C}i_L v_2 + \chi \tag{6.1.17}$$

where i_L is measured, v_2 is known, R_{L0} is a nominal value of R_L, and χ is the injection term. The dynamics of the output voltage estimation error $e_V = V_L - \hat{V}_L$ are derived

$$\frac{de_V}{dt} = \frac{V_L}{C}\left(\frac{1}{R_L} - \frac{1}{R_{L0}}\right) - \chi \tag{6.1.18}$$

The injection term that is designed in a SMC format

$$\beta = \bar{\rho}\,sign(e_V), \quad \bar{\rho} > \frac{V_L|R_L - R_{L0}|}{CR_{L0}R_L}, \quad V_L > 0 \tag{6.1.19}$$

(6.1.19) will drive $e_V \to 0$ in finite time. In the sliding mode $e_V = 0$ we obtain

$$\frac{V_L(R_L - R_{L0})}{CR_{L0}R_L} - \beta_{eq} = 0 \Rightarrow \hat{R}_L = R_{L0}\frac{V_L}{V_L - CR_{L0}\beta_{eq}} \tag{6.1.20}$$

where β_{eq} is an *equivalent* injection term [6] that can be obtained via low pass filtering of the injection term (6.1.9) in the sliding mode [6], for instance

$$\tau_1\dot{\beta}_{eq} + \beta_{eq} = \beta, \quad \tau_1 > 0 \tag{6.1.21}$$

In order to avoid a possible singularity in eq. (6.1.10), it can be regularized

$$\hat{R}_L \approx R_{L0} \frac{V_L\left(V_L - CR_{L0}\beta_{eq}\right)}{\left(V_L - CR_{L0}\beta_{eq}\right)^2 + \varepsilon}, \quad \varepsilon > 0 \tag{6.1.22}$$

The estimation error e_V can be easily driven to zero using the ASTW control in (6.1.4), (6.1.5).

Finally, the control law $u = \left[P_{O_2}, u_1, u_2\right]^T$ is designed.

6.5 Summary

The Sliding mode controller is designed accordingly for each and every component present in the fuel cell system. The dynamics of each component is analyzed carefully and the suitable controller is implemented to achieve outstanding results. In order to achieve non- overestimated control gains, adaptive gain super twisting controller is designed for the inductance current. The output voltage is controlled effectively using a traditional sliding mode controller. The ultra capacitor voltage and current are controlled efficiently using classical sliding mode control. The sliding mode observers are used in the identification of unknown load resistance. By reconstructing the unknown resistance, current command is generated.

Chapter 7

SIMULATION STUDY

In this chapter, the entire fuel cell system is studied and simulated implementing the sliding mode controller design as discussed in chapter 6. This chapter mainly discloses the simulation results discussed in previous chapters. The simulation results are progressively depicted in building the fuel cell system.

7.1 Simulation results without the ultra capacitor

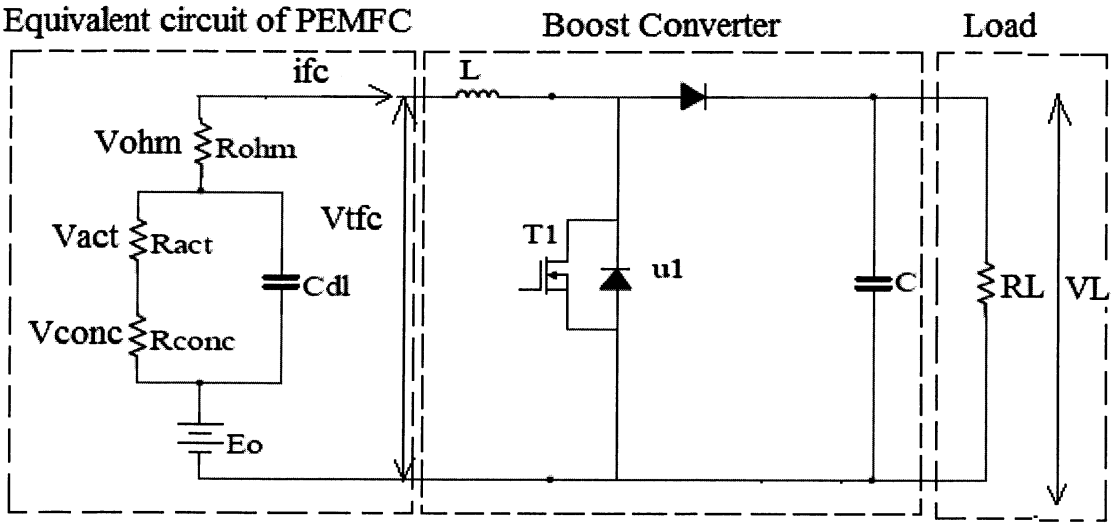

Fig.7.a. Coupling of equivalent circuit of PEMFC with the Boost converter without ultra capacitor

The system of electrical energy supply that consists of the boost DC-DC power converter, which receives a primary electrical energy from a stack of N PEMFCs and is controlled

by SMC and 2-SMC (super-twisting control), is simulated using the mathematical model in chapter 3 without implementing an ultra capacitor

The following parameters were selected during the simulations:

$$L = 7 \cdot 10^{-6} H, \quad C = C_f = 1.1 \cdot 10^{-3} F, \quad E_{fc}(0) = 24V, \quad R_{L0} = 30\Omega,$$
$$i_L(0) = 5A, \quad V_L(0) = 120V, \quad v_{fc}(0) = -0.7V$$

The following load voltage command profiles were selected in accordance with [9]-[12]

$$V_{Lc}(t) = \begin{cases} 450V, & 0 \le t \le 0.73s \\ 400V, & 0.73s < t \le 1.05s \\ 430V, & t > 1.05s \end{cases}$$

The load resistor was changed at $t = 0.83s$:

$$R_L = \begin{cases} 20\Omega, & 0 \le t \le 0.83s \\ 60\Omega, & t > 0.83s \end{cases}$$

The fuel cell varying resistor changed its value at $t = 1.05s$

$$R_{ohm} = \begin{cases} 0.5\Omega, & 0 \le t \le 1.05s \\ 0.75\Omega, & t > 1.05s \end{cases}$$

The simulation plots are presented in Figures 7.1-7.4. The plots on Fig. 8, illustrate high accuracy direct tracking of the load voltage command profile via classical sliding mode control (Fig. 7.4) in the presence of unknown changing load resistor.

From the simulation parameters, we can very well see that the voltage and current varies when there is a change in the load. The voltage and current command also varies accordingly. The estimated or the desired value at that time period is calculated and the voltage profile tracks the command or reference voltage within few seconds. The output

error tracking e1 mainly computes the difference in the desired load current and the actual current determined from the system. From the plot 8.3, it is obviously depicted that the error goes to zero in finite period of time. The output tracking error e2 elucidates the difference in the reference and actual load voltage tracking profiles. Sliding mode control enables us to design excellent error dynamics to enforce the system controllability within a short period of time. Henceforth, makes the system more efficient.

Simulation plots of the Load voltage and current control

Fig.7.1 Load voltage control

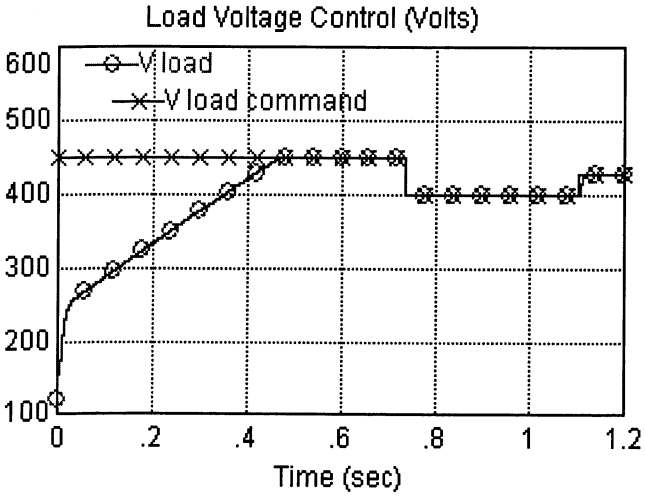

Fig.7.2 Load current control

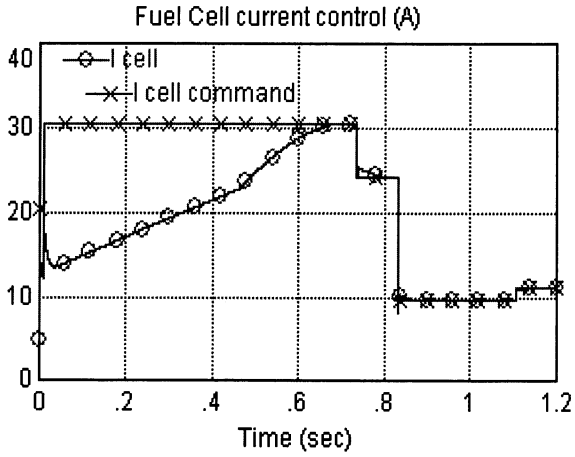

Simulation plots of output tracking errors e1 and e2 and Identification of the load resistor

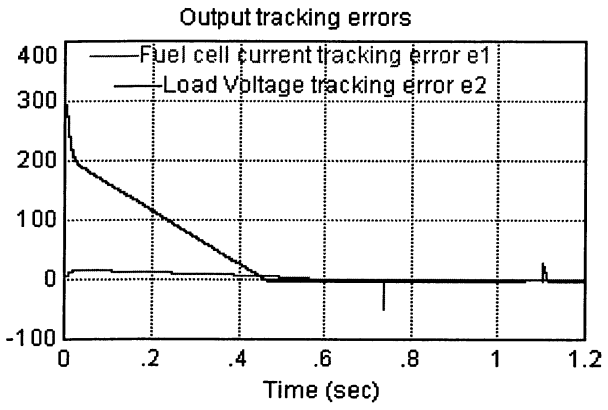

Fig.7.3 Output tracking errors

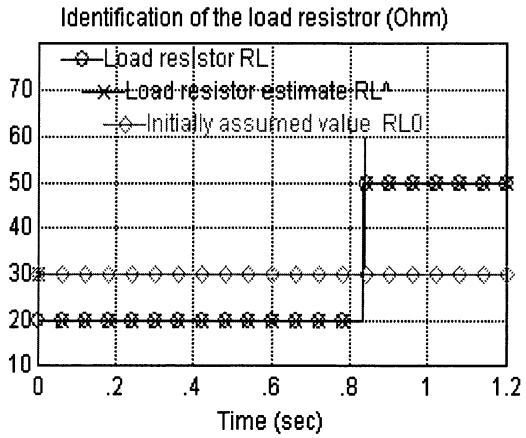

Fig.7.4 Identification of load resistor

The Sliding mode observer is used to track the load resistance. The load mainly depends on the consumer demand. The schematic shown in the figure (7.a) does not conserve any energy in the circuit. There are certain minor losses in the circuit which leads to voltage drop. Hence the efficiency is not at its maximum. The theoretical results obtained without an ultra capacitor does not completely satisfy the practical implementation of the circuit in either industrial or domestic purposes. In short, the energy is not completely conserved and if a failure occurs in in any of the components like PEMFC or the DC-DC Boost converter, the will be absolutely no supply to the load. Thereby, resulting in a power shut down. This challenge can be easily overcome by adding the ultra capacitor connected to the load of the DC-DC boost converter to improve the performance of the entire fuel cell system.

Remark

Super-twisting control is used without gain adaptation but fixed gains that have been tuned to be as,

$$\alpha = 330$$
$$\beta = 26$$

The control function ω_1 is fed directly to PEMFC neglecting the dynamics of the oxygen pump.

7.2 Simulation results with the ultra capacitor

The fuel system is built completely with the ultra capacitor and simulated for verification of the theoretical results. The ultra capacitor is advantageous in trapping the minor energy losses that take place in the circuit. It stores this energy and later discharges it, when required. The energy is efficiently managed in this system configuration shown in schematic (5.1.1).The system of electrical energy supply that consists of the boost DC-DC power converter, which receives a primary electrical energy from a stack of n PEMFCs and is controlled by SMC and ASTW control, is simulated using the mathematical model in eq. (5.1.1) and controls given by eq. (6.1.23).

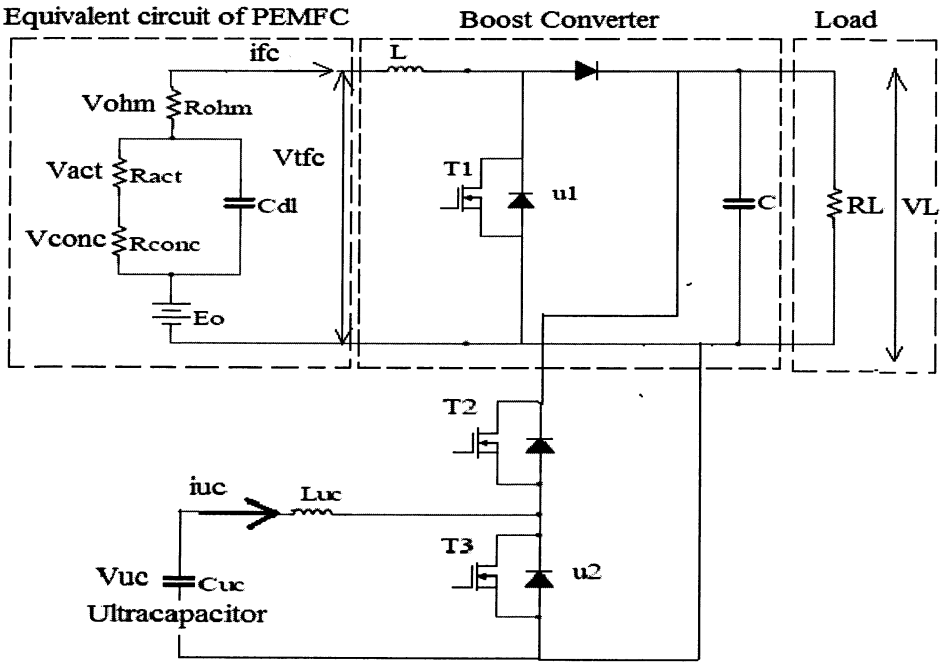

Fig.7.b. Coupling of equivalent circuit of PEMFC with the Boost converter with an ultra capacitor

The following parameters were selected during the simulations:

$$L = 7 \cdot 10^{-6} H, \quad C = C_f = 1.1 \cdot 10^{-3} F, \quad E_{ftc}(0) = 24V, \quad R_{L0} = 30\Omega,$$
$$i_L(0) = 5A, \quad V_L(0) = 120V, \quad v_{fc}(0) = -0.7V, T_{fc} = 353K, R_{ohm} = 0.06$$
$$L_{uc} = 140 * 10^{-6}$$

The simulations are carefully selected to verify the theoretical calculations. Since the ultra capacitor stores all the energy that is lost in minor ohmic loses and regenerates the same in case of power shut down. It acts as an auxiliary power supply source. The fuel cell system is controlled in spite of the uncertain parametric variations. The sliding mode control provides excellent robustness to the internal dynamics of the system (5.1.1) when subjected to disturbances without any anticipation. The Sliding Mode controller design is carefully selected to compensate and control the system dynamics. Henceforth, enables

us to achieve desired results.

L=35.10^{-6}H; C, Cdl=14.$10^{-3}F$, 68.$10^{-3}F$; $i_L(0)$=6A; $V_L(0)$=100V; R_{L0}=20-30Ω ; R_{act} =0.08;

V_{uc}=30V; C_{uc}=125F.

The following load voltage command profiles were selected in accordance with [9]-[12]

$$V_{Lc}(t) = \begin{Bmatrix} 400V, 0 \le t \le 0.75s \\ 450V, 0.75 \le t \le 1.1s \\ 400V, t > 1.1s \end{Bmatrix}$$

The load resistor was changed at $t = 0.83s$:

$$R_L = \begin{cases} 20\Omega, & 0 \le t \le 0.83s \\ 60\Omega, & t > 0.83s \end{cases}$$

The fuel cell varying resistor changed its value at $t = 1.05s$

$$R_{ohm} = \begin{Bmatrix} 0.75\Omega, 0 \le t \le 1.05s \\ 1.00\Omega, t > 1.05s \end{Bmatrix}$$

The figures 7.5 and 7.6 show the simulation plots of load voltage and current with an ultra capacitor. The figure 7.7 illustrates the working of the ultra capacitor in terms of the ultra capacitor time history. The spikes in the graph indicate the ultra capacitor charging and discharging in regular intervals of time. Figure 8.8 depicts Adaptive gain value α. The simulation plot of the adaptive gain α shows a dynamic increase initially and later starts reducing. This reduction in gain is mainly due to the establishment of the 2-Sliding mode.

Fig.7.5 Load voltage control

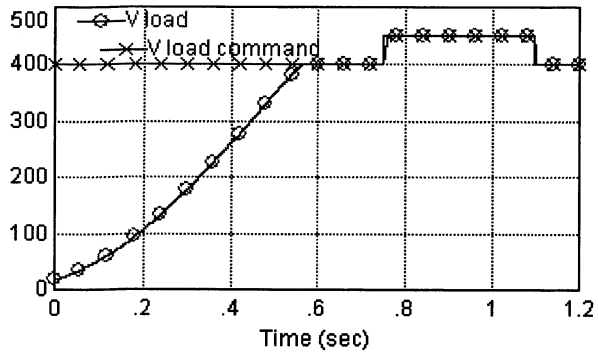

Fig.7.6 Load current control

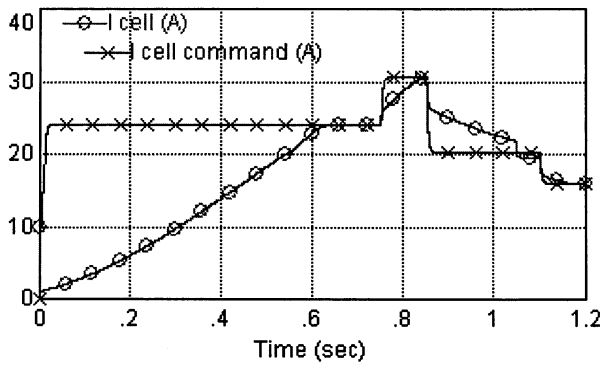

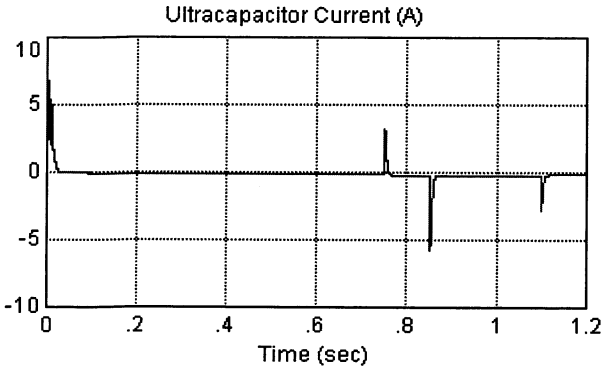

Fig.7.7 Ultra capacitor current time history

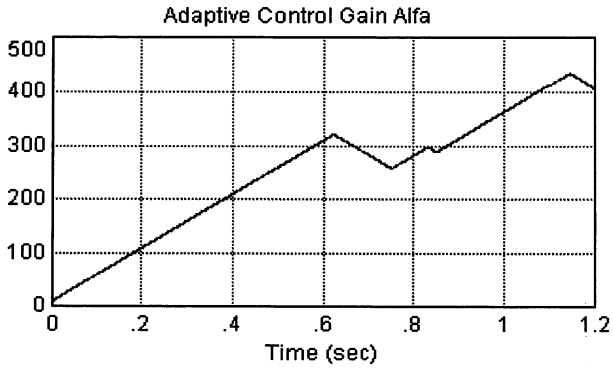

Fig.7.8 Adaptive control gain alpha

The gain α then reverses or starts increasing at time (t>0.8) seconds. This is because the sliding variable or its derivative starts start deviating from the equilibrium $\sigma = \dot{\sigma} = 0$.

Fig.7.9 Adaptive control gain Beta

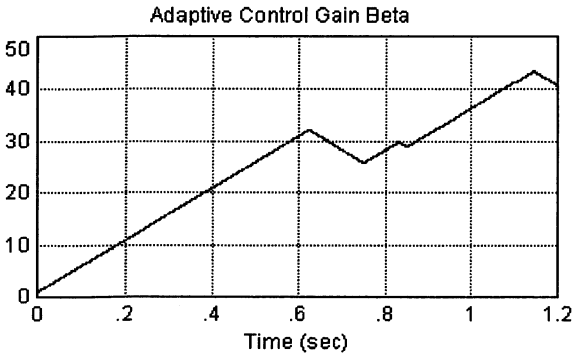

Fig.7.10 PEMFC current control ω_1

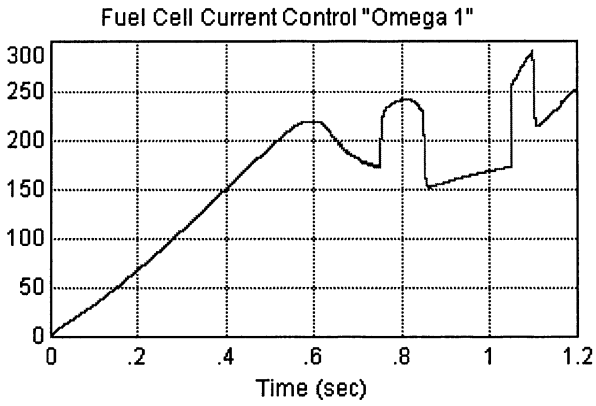

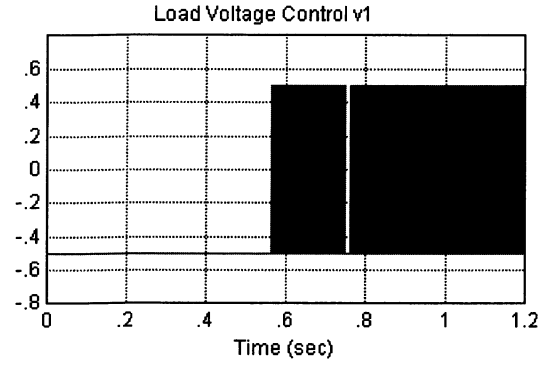

Fig.7.11. DC-DC Boost power converter control v1

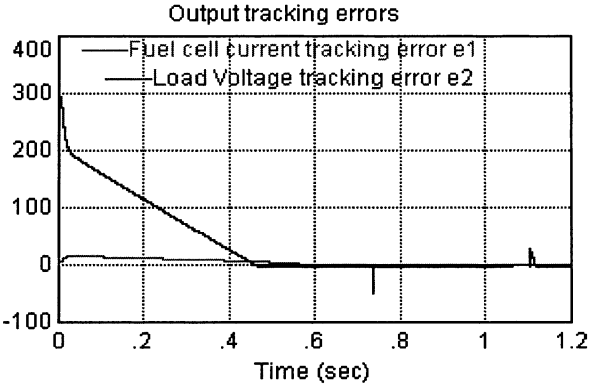

Fig.7.12Output tracking errors

The plots on Fig. 4 illustrate high accuracy direct tracking of the load voltage command profile via traditional sliding mode control (Fig. 7.5) in the presence of unknown changing load resistor that is accurately reconstructed by the sliding mode resistor observer in equations (6.1.17)-(6.1.22), while the voltage command profile is changing instantaneously twice during simulation time. High accuracy tracking of the fuel cell current command profile that is generated on line using equation(5.1.11) is confirmed via plots in Fig. (7.6).The ultra capacitor current that generates the fast portion of the load

current is shown in Fig. (7.7). The time history of adaptive control gains β and α is demonstrated in Figures 7.8 and 7.9. The control functions of the PEMFC current and DC-DC boost converter are shown in the figure 7.10 and 7.11. The Fig 7.12 denotes the output tracking error of the current and voltage profiles.

Remark

Here, we assume that any PEMFC current command can be followed by control ω_1. In reality, it is not the case, since the dynamics of the oxygen pump slows down this control. This challenge is overcome by considering ultra capacitors.

7.3 Summary

The simulation results are depicted for the fuel cell system with and without the ultra capacitor. The system replicates the load voltage and current irrespective of the ultra capacitor. The adaptive sliding mode control is implemented to estimate the gains irrespective of the uncertainties present in the system. The simulation results for the adaptive gains are also shown for better understanding. Thus the simulation results are shown progressively with respect to building the fuel cell system successively.

Chapter 8

CONCLUSION

Control of a power system that comprises Proton Exchange Membrane fuel cell (PEMFC), a boost DC-DC power converter, and an ultra capacitor is studied using sliding mode control techniques. Two types of sliding mode control (traditional SMC and adaptive-gain 2-SMC, continuous super-twisting control) are used in the same time for controlling PEMFC/ultra capacitor/boost DC-DC power converter system. It is observed that a three-fold SMC feedback control structure (adaptive 2-SMC PEMFC current and traditional SMC voltage and ultra capacitor current controllers) allows avoiding non-minimum phase property of boost DC-DC power converter, which output voltage is controlled directly, that simplifies the controller design. Use of sliding mode observer for on-line identification of the load resistance improves the robustness of the designed control system. The efficacy and robustness of the proposed SMC and 2-SMC controllers are confirmed via computer simulations.

Appendix: Fundamentals of Sliding Mode Control

In chapter 3 and 4, the boost converter and ultra capacitor dynamics were designed using Sliding mode control (SMC), without explaining the control algorithms of the SMC in detail. This chapter introduces the basic concepts of sliding mode control and observation. The main advantage of sliding mode control is its robustness to the matched bounded disturbances. This chapter begins with introducing the concepts of the sliding surface, the sliding mode and sliding mode control using a simple example.

A.1.Concepts of a sliding surface, a sliding mode and sliding mode control.

Consider a double integrated system such as following:

$$\left\{\begin{matrix}\dot{x}_1 = x_2 \\ \dot{x}_2 = u + f(x_1, x_2 t)\end{matrix}\right\}\left(\begin{matrix}x_1(0) = x_{10} \\ x_2(0) = x_{20}\end{matrix}\right) \qquad \text{(a.1.1)}$$

Where u is the control force, $f(x_1 x_2, t)$ is the disturbance. The disturbance is assumed to be bounded, i.e. $|f(x_1 x_2, t)| \le L > 0$. The problem is in designing the control function u that drives $x_1, x_2 \to 0$ as time increases in the presence of the bounded disturbance $f(x_1 x_2, t)$. Let us introduce desired compensated dynamics for system as described in equation (a.1.1). A good candidate for the desired compensated dynamics is formed of a homogeneous linear time invariant differential equation, such as:

$$\dot{x}_1 + c x_1 = 0, c > 0 \qquad \text{(a.1.2)}$$

Keep in mind that $\dot{x}_1 = x_2$. General solution of equation (a.1.2) is:

$$\begin{aligned} x_1(t) &= x_1(0)\exp(-ct) \\ x_2(t) &= \dot{x}_1(t) = -cx_1(0)\exp(-ct) \end{aligned} \tag{a.1.3}$$

The solution, obtained in equation (a.1.3), converges to 0 asymptotically and the effect of the bounded disturbance $f(x_1x_2,t)$ on the compensated dynamics is not observed. To achieve these compensated dynamics, let us introduce a variable, σ, in the state space of the system equation (a.1.1).

$$\sigma = \sigma(x_1, x_2) = x_2 + cx_1, c > 0 \tag{a.1.4}$$

The variable σ is called sliding variable. The first step to design sliding mode control, using equation (a.1.2) and (a.1.4), following equation is obtained.

$$\sigma = \sigma(x_1, x_2) = x_2 + cx_1, c > 0 \tag{a.1.5}$$

Equation (a.1.5) corresponds a straight line in the state variable space of the system (a.1.1), is called sliding surface.

Now the problem is reduced to driving the sliding variable $\sigma \to 0$ in finite time, because when σ is equal to 0, $x_2 + cx_1$ is also equal to 0 and $\dot{x}_1 + cx_1$ is also equal to 0, finally state variables x_1, x_2 keep the general solution which is shown in equation (a.1.3). This task can be achieved by applying Lyapunov function techniques to the sliding variable dynamics that are derived using equations (a.1.1) and (a.1.5).

$$\dot{\sigma} = cx_2 + f(x_1, x_2, t) + u, \sigma(0) = \sigma_0 \tag{a.1.6}$$

For the sliding variable dynamics equation (a.1.5), Lyapunov function is expressed as:

$$V = \frac{1}{2}\sigma^2 \tag{a.1.7}$$

In order to provide asymptotic stability of equation (a.1.6) about the equilibrium point $\sigma = 0$, the following conditions are satisfied

$$\begin{aligned} &a)\dot{V} < 0 \\ &b)\lim_{|\sigma|\to\infty} V = \infty \end{aligned} \tag{a.1.8}$$

The condition (b) is satisfied obviously. In order to achieve finite time convergence, part a) in equation (a.1.8) is modified to:

$$\dot{V} = \sigma\dot{\sigma} \le -\alpha V^{1/2}, \alpha > 0 \tag{a.1.9}$$

The condition shown in equation (a.1.9) is called the reachability condition in sliding mode control. Meeting the reachability condition corresponds system state variable x_1, x_2 are driven towards the sliding surface, shown in equation (a.1.5), and stay on sliding surface thereafter. Integrate equation (a.1.9) over the time interval $0 \le \tau \le t$, following equation coming up.

$$V^{\frac{1}{2}}(t) \le -\frac{1}{2}\alpha t + V^{\frac{1}{2}}(0) \tag{a.1.10}$$

Since V converges to 0 in finite time t_r, equation (a.1.10) can be rewritten as,

$$V^{\frac{1}{2}}(t_r) = 0 \le -\frac{1}{2}\alpha t + V^{\frac{1}{2}}(0) \tag{a.1.11}$$

t_r is called reaching time.

Solving equation (a.1.11), equation for t_r is obtained.

$$t_r \le \frac{2V^{\frac{1}{2}}(0)}{\alpha} \tag{a.1.12}$$

Therefore, control u which is designed to satisfy equation (a.1.8) drive sliding variable to 0 in finite time and keep them at 0 thereafter. Next part introduces how to design control u.

Control u must satisfy equation (a.1.8) to drive sliding variable to 0 in finite time and keep them at 0 thereafter, so consider for equation (a.1.8). The derivative of V is expressed as following.

$$\dot{V} = \sigma\dot{\sigma} = \sigma(cx_2 + f(x_1, x_2, t) + u) \tag{a.1.13}$$

Let assume control u is expressed as following equation.

$$\begin{aligned} u &= u_1 + u_2 \\ u_1 &= -cx_2 \end{aligned} \tag{a.1.14}$$

Substituting equation (a.1.13) into equation (a.1.12), equation (a.1.12) can be rewritten as follows,

$$\dot{V} = \sigma(f(x_1, x_2, t) + u_2) \tag{a.1.15}$$

$f(x_1, x_2, t)$ is bounded by L, and cx_2 is also bounded since the general solution of x_2 for sliding variable dynamics is bounded by initial value of x_2. This is obtained from equation (A.1.1) and (A.1.3). Therefore, equation (A.1.14) can be rewritten as following.

$$\begin{aligned} \dot{V} &\le |\sigma|.|f| + \sigma u_2 \le |\sigma|.L + \sigma u_2 \\ &= |\sigma|(L + sign(\sigma)u_2) \end{aligned} \tag{a.1.16}$$

Consider equation (A.1.6), condition shown in equation (A.1.8) can be expressed as following.

$$\dot{V} \le -\alpha V^{1/2} = -\frac{\alpha}{\sqrt{2}}|\sigma|, \alpha > 0 \tag{a.1.17}$$

Compare equation (A.1.15) and (A.1.16), following expression is obtained.

$$\dot{V} \le -|\sigma|(L + sign(\sigma)u_2) = -\frac{\alpha}{\sqrt{2}}|\sigma| \tag{a.1.18}$$

Solve the equation (3.17) for control gain ρ.

$$\rho = L + \frac{\alpha}{\sqrt{2}} \tag{a.1.19}$$

Finally control u is

$$\begin{aligned} u &= -\rho sign(\sigma) \\ \rho &= L + \frac{\alpha}{\sqrt{2}} \end{aligned} \tag{a.1.20}$$

The control u drives sliding variable to 0 in finite time and keep them at 0 thereafter, and state variables x_1, x_2 are driven to 0 asymptotically in a presence of the bounded disturbance. This control is called sliding mode control, and hence proved that sliding mode control is robust to the bounded disturbance. The control which is given in (a.1.20) is called traditional sliding mode control

Example 1:

The results of the simulation of system (a.1.1) with the traditional sliding mode control law (a.1.20), with initial conditions, $x_{10} = 2, x_{20} = -1$, the parameter $c = 2, \rho = 5$ and the disturbance $f(x_1, x_2, t) = \sin 2t$, are presented in Figure a.1-a.5

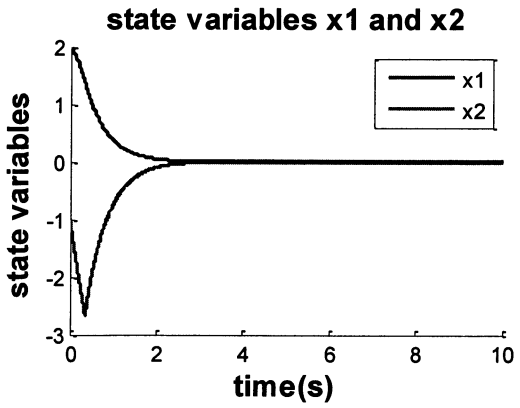

Figure a.1: State variables of Example 1

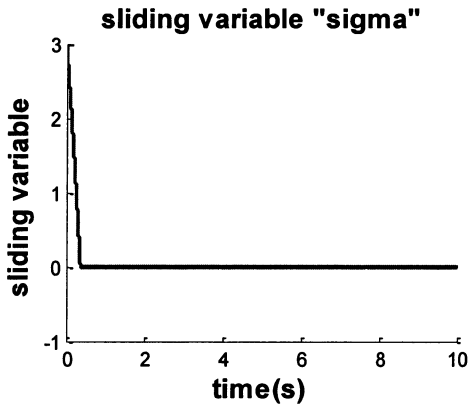

Figure a.2: Sliding variable tracking of Example 1

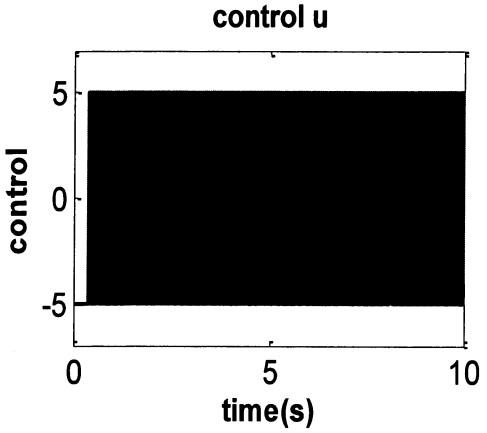

Figure a.3: Control u of example 1 ($\rho = 5$)

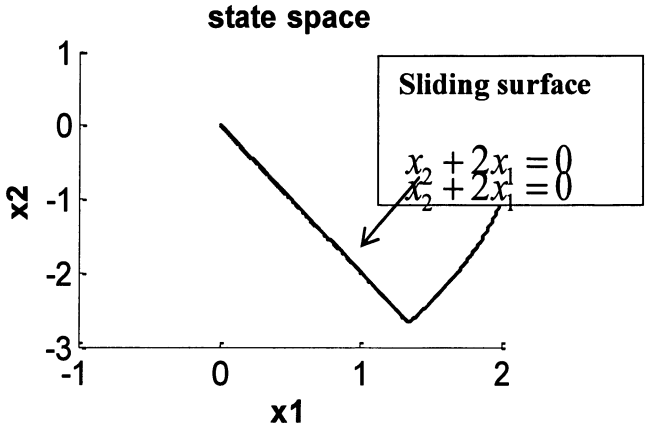

Figure a.4: State space of x_1 and x_2 of Example 1

x_1 and x_2 are driven to 0 in finite time and keep them at 0 thereafter in presence of the bounded disturbance.

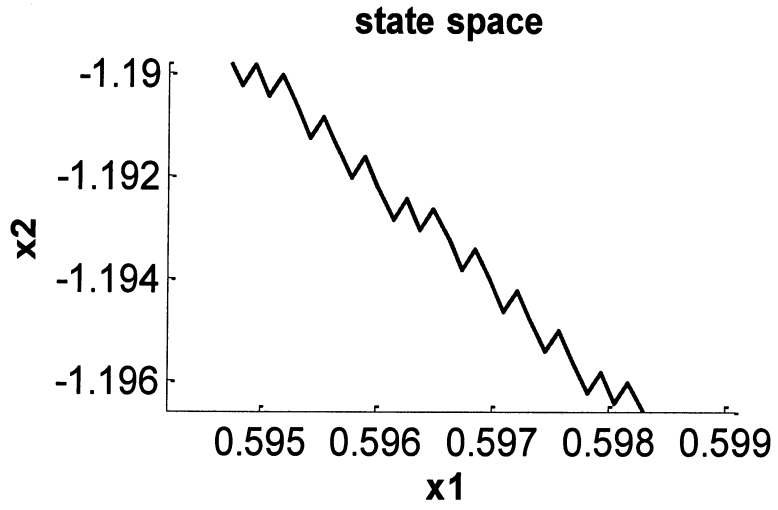

Figure a.5: Zoom of sliding surface of Figure 5

The high frequency switching control would produce a chattering motion in output. Chattering effect prevents sliding variable from converging to 0. In addition, high frequency switching control is not acceptable for actual components. The control might cause serious damage to the actual material if it is applied. Following section, introduces chattering attenuation procedure.

A.1.1 Chattering attenuation using sigmoid function

Sigmoid function is approximation of sign function. That is introduced as:

$$sign(\sigma) \approx \frac{\sigma}{|\sigma| + \varepsilon}, \tag{a.1.21}$$

where ε is a small positive number

Eliminating sign function in control u using equation (a.1.21), discontinuous control u become continuous. However, robustness of control and accuracy are lost.

Example 2: The results of example 1, with $u = -\rho \frac{\sigma}{|\sigma| + \varepsilon}, \rho = 5$

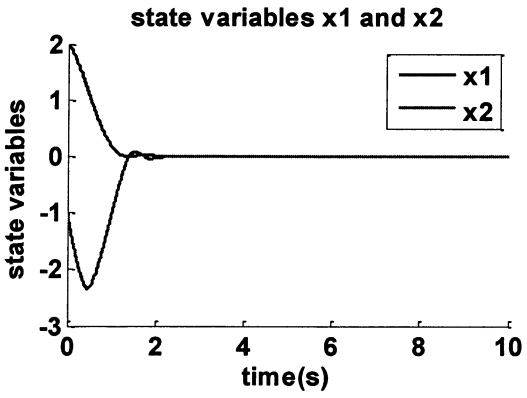

Figure a.6: State variables versus time(s)

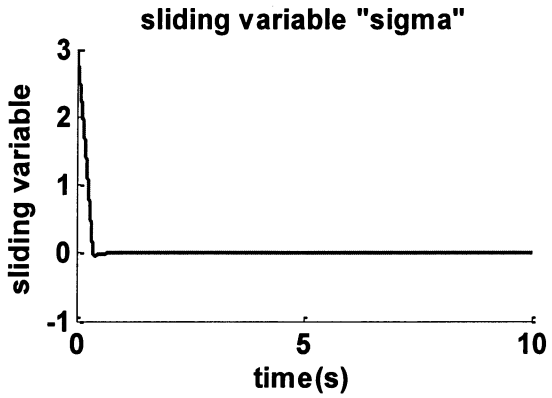

Figure a.7: Sliding variable versus time(s)

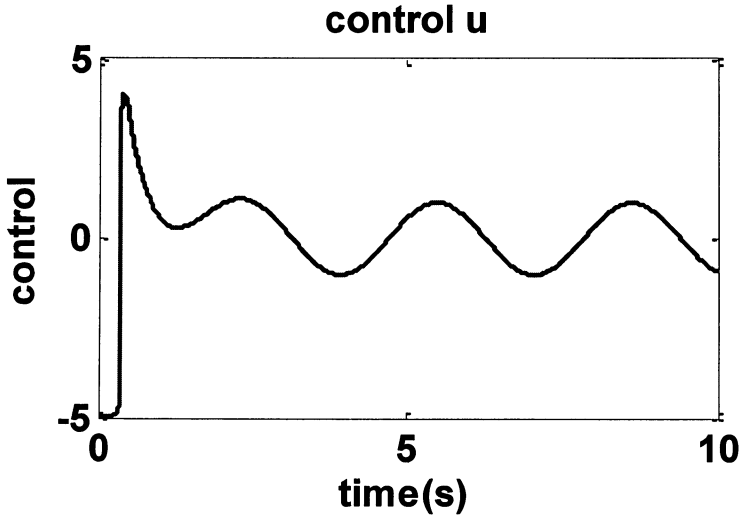

Figure a.8: Control u versus time(s)

To see the results, sliding variable converges to 0 though it oscillates. It is obvious that the sigmoid function loses the accuracy.

A.1.2 Chattering attenuation: asymptotic sliding mode

Chattering attenuation idea is to design derivative of control by means of asymptotic sliding variable. Consider system (a.1.1) again, and keep in mind that sliding variable given in equation (a.1.4) converges to 0 in finite time and state variables x_1, x_2 are also converge to 0 asymptotically in finite time in a presence of bounded disturbance. It is necessary to add a condition for this assumption.

$$\left|\dot{f}(x_1, x_2, t)\right| \leq \bar{L} \tag{a.1.22}$$

Consider an auxiliary sliding variable S introduced as following.

$$S = \dot{\sigma} + \bar{c}\sigma \tag{a.1.23}$$

Control u exists in this auxiliary sliding variable S, thereby driving S to 0 in finite time and keeps auxiliary sliding variable 'S' at 0 thereafter. Ideal sliding mode occurs in the sliding surface of $S=0$. Therefore sliding surface of S is expressed as following.

$$S = \dot{\sigma} + \bar{c}\sigma = 0 \tag{a.1.24}$$

Sliding variable σ and state variables x_1, x_2 converges to 0 as time increases in presence of the bounded disturbance. Doing same procedure as the beginning of this chapter, control u is obtained. Using equation (a.1.9) and (a.1.17), following expression is obtained.

$$S\dot{S} \leq -\frac{\alpha}{\sqrt{2}}|S| \tag{a.1.25}$$

where $S\dot{S}$ is expressed as following.

$$S\dot{S} = S[\dot{u} + \dot{f}(x_1, x_2, t) + (c + \bar{c})\{u + f(x_1, x_2, t)\} + c\bar{c}x_2] \tag{a.1.26}$$

Now assume the derivative of control u is:

$$u = -\rho sign(S), \rho > 0 \tag{a.1.27}$$

Assuming the boundary of control u is K. Then following inequality is obtained.

$$S\dot{S} \le |S|[-\rho + \bar{L} + (c+\bar{c})(K+L) + c\bar{c}x_{20}] \tag{a.1.28}$$

where x_{20} is initial condition of state variable x_2.

$$S\dot{S} \le |S|[-\rho + \bar{L} + (c+\bar{c})(K+L) + c\bar{c}x_{20}] = -\frac{\alpha}{\sqrt{2}}|S| \tag{a.1.29}$$

Then the control gain ρ is obtained.

$$\rho = \bar{L} + (c+\bar{c})(K+L) + c\bar{c}x_{20} + \frac{\alpha}{\sqrt{2}} \tag{a.1.30}$$

Finally control u is expressed as following

$$u = -\int \rho sign(S)dt, \rho = (c+\bar{c})(K+L) + c\bar{c}x_{20} + \frac{\alpha}{\sqrt{2}} + \bar{L} \tag{a.1.31}$$

Example 3:

Consider Example 1 with control

The results of the simulation of system (a.1.1) with the asymptotic sliding mode control law (a.1.31), with initial conditions, $x_{10} = 2, x_{20} = -1$, and the disturbance $f(x_1, x_2, t) = \sin 2t$, are presented in Figure a.9-a.12.

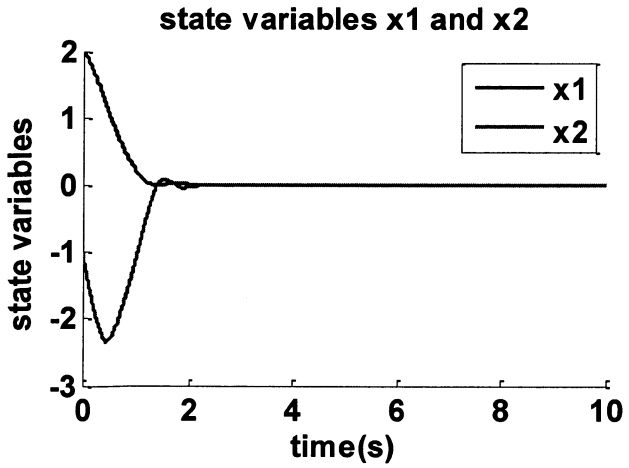

Figure a.9: State variables versus time

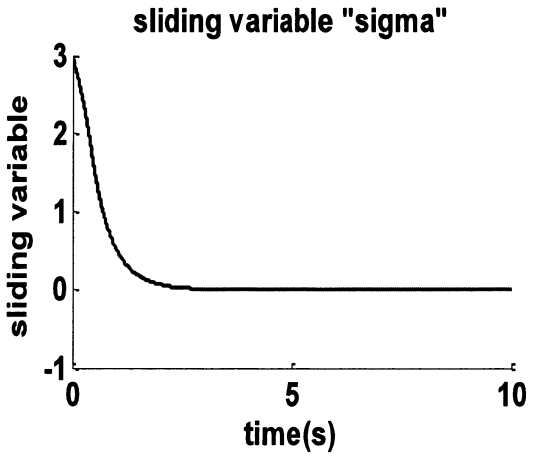

Figure a.10: Sliding variable versus time

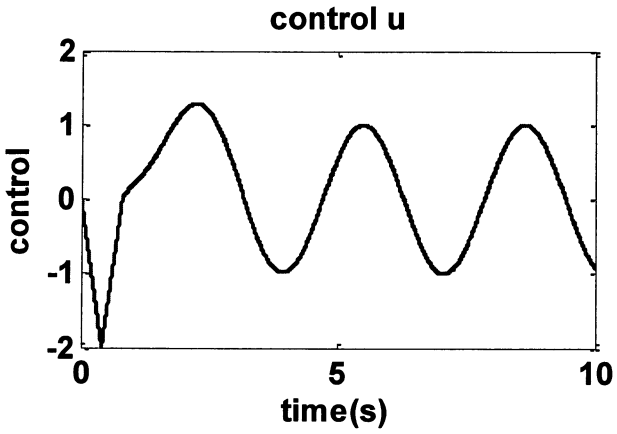

Figure a.11: Control u versus time(s)

When sliding variable is compared to the sigmoid function, asymptotic sliding mode is much accurate. Sliding variable converges to 0 without any oscillation. The control function becomes continuous.

A.2 Higher Order Sliding Mode Control and Second Order Sliding Mode Control

In previous section, the concept of sliding mode control is introduced [30]. The control u is obtained in equation (a.1.20),thereby driving sliding variable σ for system (a.1.1) to 0 in finite time and keeps the sliding variable at 0 thereafter in the presence of the bounded disturbance. Higher order sliding mode control is control u, which drives sliding variable and r-1times derivative of sliding variable of a system to 0 in finite time and keep them at 0 thereafter in a presence of disturbance.

If the condition is met in finite time,

$$\sigma = \dot{\sigma} = ... = \sigma^{(r-1)} = 0, \tag{a.1.32}$$

Then r-th order sliding mode control exists in system (a.1.33).

$$\sigma^{(r)} = \varphi + gu, |\varphi| \le L, g \in [K_m, K_M] \tag{a.1.33}$$

The control function u that drives $\sigma = \dot{\sigma} = ... = \sigma^{(r-1)} = 0,$ in system (a.1.33) to zero in finite and keeps them there is called higher order sliding mode control (HOSM). Advantages using higher order sliding mode is possibility for continuous, chattering attenuation and talent for arbitrary relative degree. When relative degree is 2, that is called second order sliding mode. Fundamentals of second order sliding mode control, twisting control and super-twisting control is introduced in following subsections.

A.2.1 Fundamentals of second order sliding mode control

Consider (a.1.33) for r=2:

$$\sigma^{(2)} = \varphi + gu \tag{a.1.34}$$

The following condition for equation (a.1.34) is assumed to be met.

$$0 < K_m \le \frac{\partial}{\partial u}\ddot{\sigma} \le K_M, \left|\ddot{\sigma}\right|_{u=0} \le C \tag{a.1.35}$$

Where $K_m, K_M and C$ are certain positive constants. Where u is second order sliding mode control and σ is sliding variable. Then equation (a.1.34) can be rewritten in terms of differential inclusions

$$\ddot{\sigma} \in [-C, C] + [K_m, K_M]u \tag{a.1.36}$$

Second order sliding mode controllers are considered as a control which drives sliding variable and its first derivative to 0 in finite time and keeps them at 0 thereafter in the presence of the bounded disturbance. Second order sliding mode control is robust to any bounded perturbations.

A.2.2 Super-twisting control (STW)

Super-Twisting control is a continuous second order sliding mode control [30]. This approach is effective for relative degree 1. The advantage of this control technique is to eliminate chattering. In other words, super-twisting control stabilizes sliding variables robustly at 0 in finite time for any bounded disturbance.

The relative degree 1, sliding variable dynamics for super-twisting control is given to be as follows

$$\dot{\sigma} = \varphi + gu \tag{a.1.37}$$

where $|\dot{\varphi}| \le C, 0 \le K_m \le g \le K_M$ .For the sliding variable dynamics given in (a.1.37), super-twisting control is introduced as:

$$\left\{ \begin{array}{l} u = -c|\sigma|^{1/2} sign(\sigma) + \varpi \\ \dot{\varpi} = -bsign(\sigma) \end{array} \right\} \tag{a.1.38}$$

where $1.5\sqrt{C}, b = 1.1C$

This super-twisting control makes the compensated dynamics of sliding variables as follows:

$$\dot{\sigma} + c|\sigma|^{1/2} sign(\sigma) + b\int sign(\sigma)dt = \varphi \tag{a.1.39}$$

In sliding mode, $b\int sign(\sigma)dt = \varphi$ reaches in finite time. The super-twisting control function (a.1.38) drives both σ and $\dot{\sigma}$ to zero in finite time and keeps them at 0 thereafter.

Example 4:

The results of the simulation of system (a.1.1) with the super-twisting control law (a.1.38) and (a.1.39), with initial conditions $x_{10} = 2, x_{20} = -1$, the parameter $\sigma = x_2 + 2x_1, C = 5$ and the disturbance, $f(x_1, x_2, t) = \sin 2t$ are presented in Figure a.13-a.15.

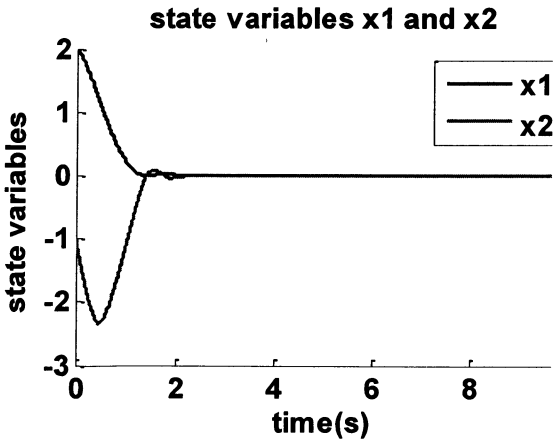

Figure a.12: State variable versus time with STW

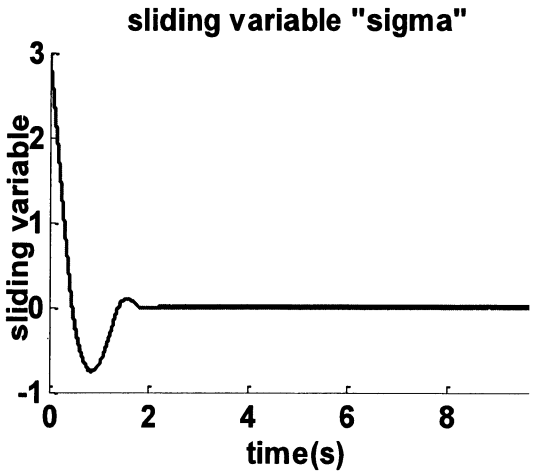

Figure a.13: Sliding variable versus time(s) with STW

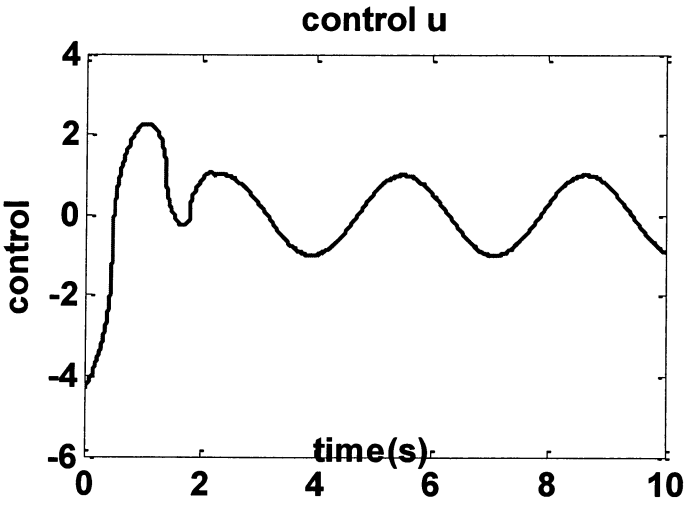

Figure a.14: Control u versus time(s)

A.3 Sliding Mode Observer/Differentiator

In previous sections, state variables are assumed as measurable. But, in some case, only x_1 is measurable and $x_2$is estimated. In this section, the state variables are estimated using sliding mode observers. Traditional sliding mode observer and super-twisting observer are the two types of the sliding mode observer. This section introduces sliding mode observer using system (a.1.1)

A.3.1 Traditional sliding mode observer /differentiator design

Consider system (a.1.1),

$$\left.\begin{cases} \dot{x}_1 = x_2 \\ \dot{x}_2 = u + f(x_1, x_2 t) \end{cases}\right\} \begin{pmatrix} x_1(0) = x_{10} \\ x_2(0) = x_{20} \end{pmatrix}$$

Assume state variable x_1 is measurable, x_2 is not measurable, and disturbance $f(x_1, x_2, t)$ is bounded. The first step of design of sliding mode control is to design sliding variable. In the beginning of this chapter, sliding mode control is designed using sliding variable dynamics (3.4). However, the sliding variable dynamics has a term of x_2. Since x_2 is not measurable, x_2 is needed to be estimated. To estimate x_2, let assume

$$\dot{\hat{x}}_1 = v \tag{a.1.41}$$

Where $\hat{x}_1$ is estimated value of x_1 and where v is an observer injection term. v is designed so that $\hat{x}_1, \hat{x}_2 \to x_1, x_2$. Keep in mind that $\dot{\hat{x}}_1 = \hat{x}_2$ since $\dot{x}_1 = x_2$.

Auxiliary sliding variable for sliding mode observer is defined as:

$$z_1 = \hat{x}_1 - x_1 \tag{a.1.42}$$

Then derivative of (6.1.42) is derived to be as follows,

$$\dot{z}_1 = -x_2 + v \tag{a.1.43}$$

Selecting the injection term v that drives $z_1 = \hat{x}_1 - x_1 = 0$ in finite time.

$$v = -\rho sign(z_1), \rho > |x_2| + \beta, \beta > 0 \tag{a.1.44}$$

Then reachable condition is expressed as following.

$$z_1 \dot{z}_1 = z_1(-x_2 - \rho sign(z_1)) \leq |z_1|(|x_2| - \rho) \leq -\beta |z_1| \tag{a.1.45}$$

Equation (a.1.42) means z_1 converges to 0 in finite time t_r

$$t_r \leq \frac{|z_1(0)|}{\beta} \tag{a.1.46}$$

This equation is obtained by deriving the dynamics of the sliding mode observer equation

$$\dot{z}_1 = -x_2 + v_{eq} = 0 \tag{a.1.47}$$

The concept of equivalent control is the average effect of the high frequency switching control. Equivalent control is obtained by low pass filtering of high frequency switching term, i.e. $sign(x)$ of control.

Equation (a.1.44) can be rewritten as:

$$x_2 = v_{eq,} t \geq t_r \tag{a.1.48}$$

Then the injection term v_{eq} is estimated by low pass filtering of v . τ is a small positive constant.

$$\hat{v}_{eq} = \frac{1}{\tau s + 1} v \tag{a.1.49}$$

Then x_2 is estimated after the transient response in the low pass filter(6.1.49) is over.

$$x_2 \approx \hat{x}_2 = \hat{v}_{eq}, t \geq t_r \tag{a.1.50}$$

Example 5:

Consider example 1, assume x_2 should be estimated. In this example, using sliding mode observer, estimate x_2, then drive state variable to 0 in finite time in the presence of the bounded disturbance, using traditional sliding mode control, $u = -5 \cdot sign(\sigma)$.The variable x_2 is estimated using the sliding mode observer (a.1.49), (a.1.52), (a.1.57) and (a.1.58) with $\rho = 10$and $\tau = 0.00001$. The results show in Figures. a.19-a.23.

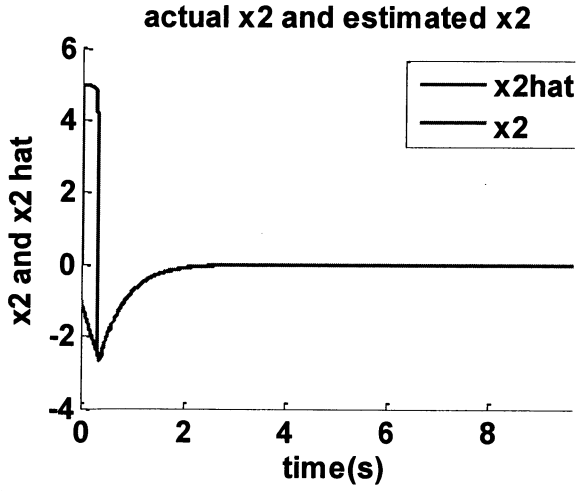

Figure a.15: x_2 and estimated x_2 versus time

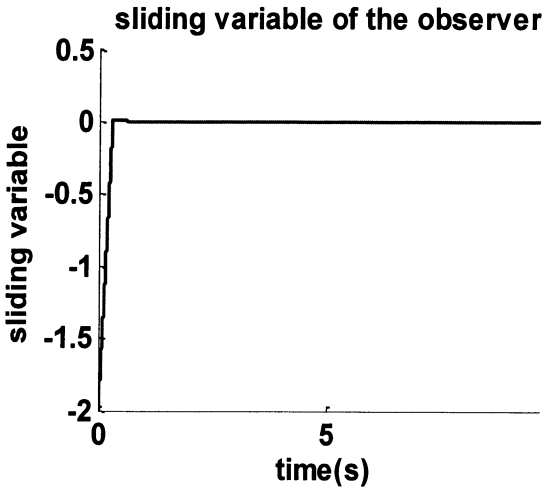

Figure a.17: Sliding variable of observer versus time

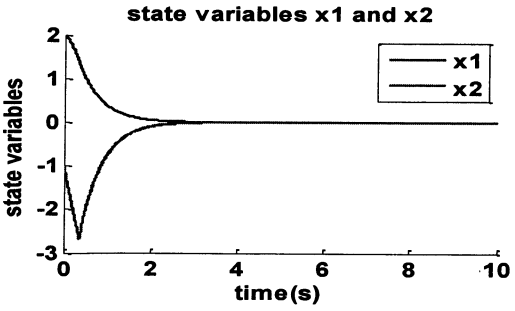

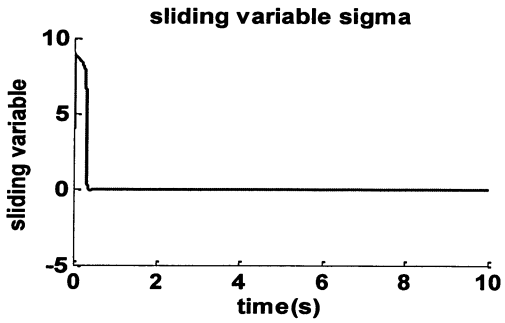

Figure a.16: State variables x_1 and x_2 versus time

Figure a.18: Sliding variable sigma versus time

A.3.2 Super-twisting observer/differentiator

Using super-twisting control law, we design ν to drive $z_1 = \widehat{x_1} - x_1 \rightarrow 0$ in finite time. As presented in chapter (a.2.3), super-twisting control law is defined as following.

$$\begin{aligned} v &= -c|z_1|^{\frac{1}{2}} sign(z_1) - \omega, \\ \dot{\omega} &= bsign(z_1) \end{aligned} \tag{a.1.51}$$

Gain value for sliding mode observer is in condition shown as follows.

$$c = 1.5\sqrt{C}, b = 1.1C, C > |\dot{x}_2| \tag{a.1.52}$$

Super-twisting control law is continuous function as explained in chapter (a.2.3). The equation (a.1.58) estimates $x_2$accurately. Therefore,

$$x_2 \approx \hat{x}_2 = v, t \geq t_r \tag{a.1.53}$$

Then, z_1 converges to 0 in finite time, and $\widehat{x_1} \rightarrow x_1$.

Example 6:

Consider example 1, assume x_2 should be estimated. In this example, using super-twisting sliding mode observer, estimate x_2, then drive state variable to 0 in finite time in the presence of the bounded disturbance, using traditional sliding mode control, $u = -\rho \cdot$

$sign(\sigma)$, $\rho = 5$ and super-twisting observer $v = -c|z_1|^{\frac{1}{2}}sign(z_1) - b\int sign(z_1)dt$, where $c = 1.5\sqrt{C}$, $b = 1.1C$, $C = 5$.

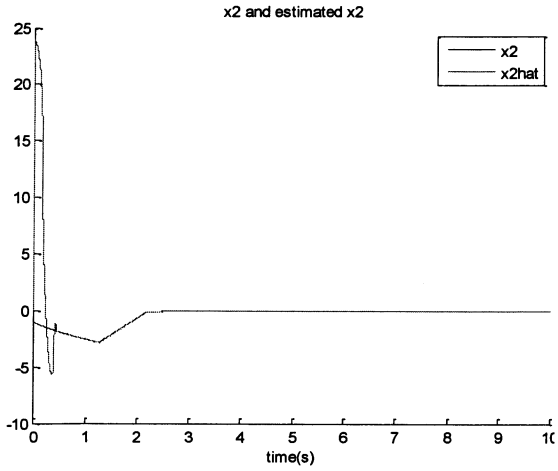

Figure a.19: x_2 and estimated x_2 versus time

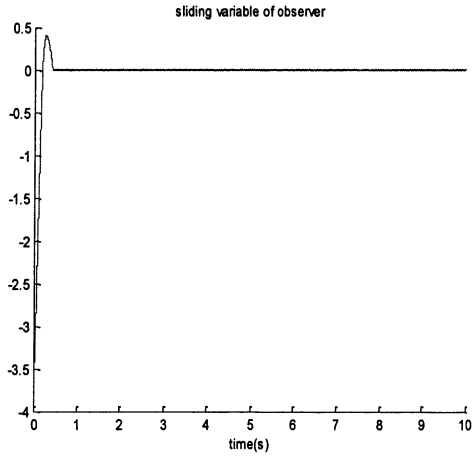

Figure a.20: Sliding variable for observer

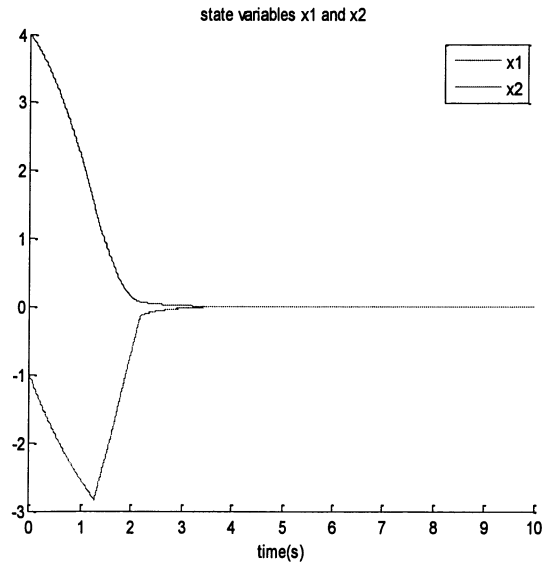

Figure a.21: State variables versus time

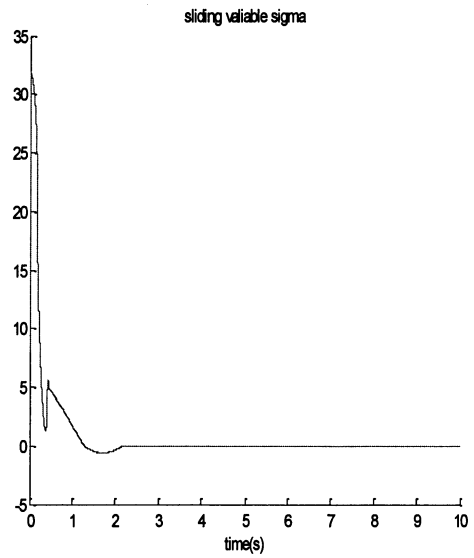

Figure a.22: Sliding variable σ

A.4 Adaptive Sliding Mode Control

In previous sections, we discussed the sliding mode control design of a certain system with the bounded disturbances which boundary is known. In this section, sliding mode control design when the boundary of the disturbances in a system is unknown, is discussed. Actually, it is possible to design sliding mode control with the large control gain, however, overestimating of the sliding mode control gain can result increased chattering. Gain adaptation is one of way to fix overestimation by adjusting the control gain dynamically.

A.4.1 Adaptive traditional sliding mode control (ATSMC)

In this section, the concept and design process of gain adaptation for traditional sliding mode control is introduced.

Two adaptive sliding mode controllers have been proposed in Lee and Utkin [6] and Huang et al [5]. The difference between those adaptive sliding mode control, is the first does not require the knowledge of the boundary of the uncertainties/perturbations and consists in increasing the control gain until the sliding mode is established, while the second one requires the knowledge of the boundary of the uncertainties/perturbations and is using the equivalent control concept in order to evaluate and to minimize the control gain.

The gain adaptation that is introduced in [5] is discussed below,

The nonlinear uncertain system

$$\begin{aligned} \dot{x} &= f(x) + g(x)u \\ \sigma &= \sigma(x) \end{aligned} \qquad \text{(a.1.54)}$$

with $x \in \mathbb{R}^n$ the state vector, $u \in \mathbb{R}^1$ the control function and $\sigma = \sigma(x) \in \mathbb{R}^1$ is the sliding variable of relative degree 1. Vector fields $f(x) \in \mathbb{R}^n$ and $g(x) \in \mathbb{R}^n$ are uncertain and norm-bounded. The control objective is to drive the sliding variable to 0. The sliding variable dynamics are defined as follows:

$$\dot{\sigma} = \psi(x,t) + \Gamma(x,t)u \qquad \text{(a.1.55)}$$

where $\psi(x,t)$ and $\Gamma(x,t)$ are assumed to be bounded: $|\psi(x,t)| \le \bar{\psi}$ and $|\Gamma(x,t)| \in [\bar{\Gamma}_1, \bar{\Gamma}_2], 0 < \bar{\Gamma}_1 < \bar{\Gamma}_2$ The boundaries $\bar{\psi}$ and $\bar{\Gamma}$ exist but are not known.

The system (a.1.54) with the sliding variable dynamics (a.1.55) is controlled by

$$u = -K(t)sign(\sigma(x,t)) \tag{a.1.56}$$

with the gain adaptation $K(t)$ given by

$$\dot{K} = \bar{K}.|\sigma(x,t)| \tag{a.1.57}$$

where $\bar{K} > 0$ and $K(0) > 0$, then the state variable converges to 0 in finite time in the presence of the bounded uncertainties/disturbances.

The main feature of this approach is that it does not require the knowledge of the boundary of the uncertainties/disturbances. However, there is a great risk of the control gain being overestimated by the gain adaptation (a.1.57), as a result, increased chattering is caused.

The gain adaptation law that is introduced in [28,29] is discussed as follows,

The given system (a.1.55) with the sliding variable dynamics (a.1.56) is controlled by

$$u = -K(t)sign(\sigma(x,t)) \tag{a.1.58}$$

The gain-adaptive SMC algorithm that allows the gain to get reduced (not to be overestimated) that yield chattering reduction is proposed in the work [28,29].

The adaptive-gain SMC given by (a.1.58)with the gain $K(t)$ defined such that

$$\dot{K} = \begin{cases} \bar{K}|\sigma(x,t)|sign(|\sigma(x,t)| - \varepsilon) \cdots if(K > \mu) \\ \mu \ldots if(K \leq \mu) \end{cases} \qquad \text{(a.1.59)}$$

where $K(0)>0$, $\bar{K} > 0$, $\varepsilon > 0$ *and* $\mu > 0$. μ is very small constant is proposed [28,29]. The parameter μ is introduced in order to keep positive values for K.

When σ is a large value, $\dot{K}$ becomes large, thereby increasing K rapidly. Similarly When $|\sigma|$ becomes smaller than ε value, $\dot{K}$ is a negative thereby K decreases slowly. Gain adaptation function changes the sign and slope of K raises positive to negative and vice-versa, on the boundary of $|\sigma| - \varepsilon = 0$. When K is smaller than μ, K increase in the slope of μ.

Example 7:

The results of the simulation of system (a.1.54) with the adaptive traditional sliding mode control law (a.1.64)-(a.1.65), with initial conditions $x_{10} = 2$, $x_{20} = -1$, the parameter$\bar{K} = 5$, $\epsilon = 0.1$, $\mu = 1$and the disturbance $f(x_1, x_2, t) = sin2t$, are presented in Figure a.25-a.28.

As a result, state variables and sliding variable converges to 0 in finite time in presence of the disturbance, and the control gain is decreasing.

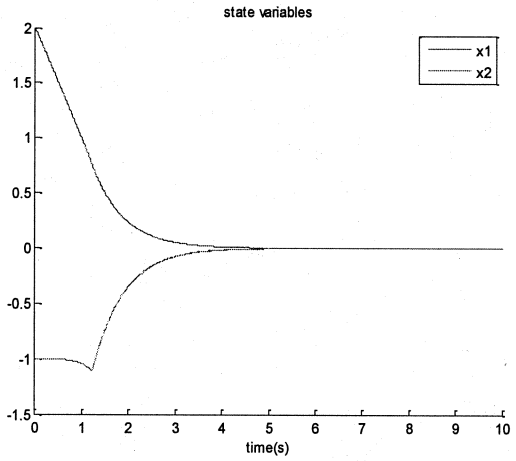

Figure a.23: Depiction of state variables versus time using ATSMC

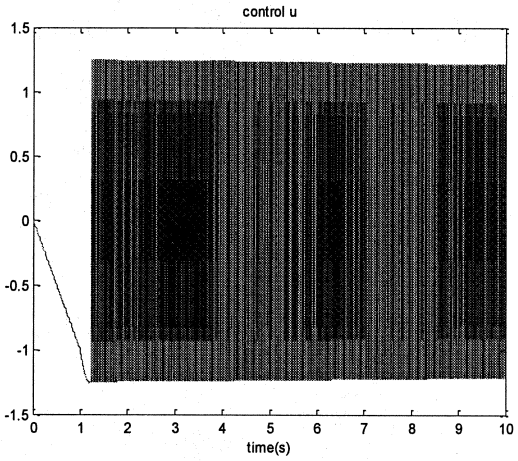

Figure a.26: Control *u* versus time using ATSMC

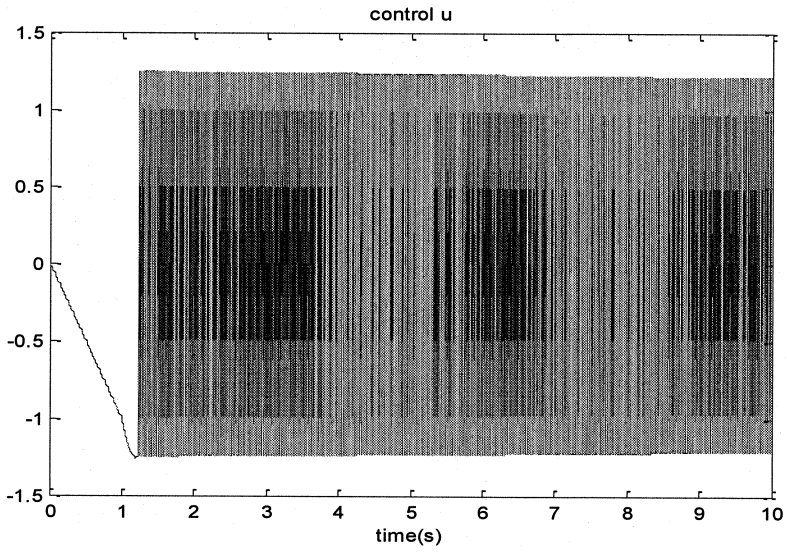

Figure a.24: Control *u* versus time using ATSMC

A.4.2 Adaptive-gain 2-SMC (super-twisting) control (ASTW)

The adaptive-gain 2-SMC super-twisting algorithm drives the sliding variable and its derivative to zero in finite time in the presence of bounded disturbances which bounds are unknown. The other advantage of the proposed adaptive 2-SMC algorithm is in achieving non-overestimated control gains that reduce chattering.

Consider the sliding variable dynamics

$$\dot{\sigma} = a(t,x) + \varpi_1 \tag{a.1.60}$$

where $\sigma, a, \omega_1 \in \mathbb{R}$, $x \in \mathbb{R}^n$, ω_1 is a control function, $a(t,x) = a_1(t,x) + a_2(t,x)$ with bounded a_1, a_2 : and $\delta_1, \delta_2 > 0$ are supposed to exist but unknown.

$$|a_1(t,x)| \le \delta_1 |\sigma|^{1/2}, \quad |\dot{a}_2(t,x)| \le \delta_2 \tag{a.1.61}$$

The adaptive gains are given to be as follows,

$$\alpha = \alpha(\sigma, \dot{\sigma}, t), \quad \beta = \beta(\sigma, \dot{\sigma}, t) \tag{a.1.62}$$

The adaptive super-twisting (ASTW) control [5] are defined in the following theorem [16]

$$\begin{aligned} \varpi_1 &= -\alpha |\sigma| sign(\sigma) + \varpi_2 \\ \dot{\varpi}_2 &= -\frac{\beta}{2} sign(\sigma) \end{aligned} \tag{a.1.63}$$

Theorem 1. *Consider system (7.1.1). Suppose that the functions* $a_1(t,x), a_2(t,x)$ *satisfy conditions (7.1.2) for some unknown gains* $\delta_1, \delta_2 > 0$. *Then, for any initial conditions*

$x(0), \sigma(0)$, *there exist a finite time* $t_F > 0$ *and a parameter* $\mu > 0$ *(as soon as the following condition holds if* $|\sigma(0)| > \mu$*)*

$$\alpha > \frac{1}{\lambda}\left[\delta_1\left(\lambda + 4\varepsilon^2\right) + \varepsilon\left(\delta_2 + 1\right) + \frac{1}{4\varepsilon}\left(2\varepsilon\delta_1 + \frac{\delta_2}{2} - \lambda - 4\varepsilon^2\right)^2\right]$$

so that real 2-sliding mode, i.e. $|\sigma| \le \eta_1, |\dot{\sigma}| \le \eta_2$, *is established for* $t \ge t_F$ *via adaptive super-twisting control (7.1.4) with the adaptive gains*

$$\begin{aligned} \dot{\alpha} &= \begin{cases} \frac{\varpi}{\sqrt{2}} sign\left(|\sigma| - \mu\right), & if \ \alpha > \alpha_m \\ \eta, & if \ \alpha \le \alpha_m \end{cases} \\ \beta &= 2\varepsilon\alpha, \quad \alpha(0) > \alpha_m \end{aligned} \tag{a.1.64}$$

where $\varepsilon, \lambda, \eta$ *are arbitrary positive constants,* $\eta_1, \eta_2 > 0$ *and* α_m *is an arbitrary small positive constant.*

The idea of designing ASTW is to dynamically increase the control gains $\alpha(t)$ and $\beta(t)$ until the 2-sliding mode establishes. Then the gains shall start reducing. This gain reduction shall be reversed as soon as the sliding variable or its derivate start deviating from the equilibrium point $\sigma = \dot{\sigma} = 0$ in 2-sliding mode. Therefore, a rule (a detector) that detects the beginning of a destruction of the sliding mode shall be constructed and incorporated in the ASTW control law that allows not-overestimating the control gains $\alpha(t)$ and $\beta(t)$ .This "detector" is proposed to design by introducing a domain $|\sigma| \le \mu$ that is used as follows: as soon as this domain is reached the gains $\alpha(t)$ and $\beta(t)$ start

dynamically reducing until the system trajectories leave the domain. Then the gains start dynamically increasing in order to force the trajectories back to the domain in finite time.

A.5 Summary

In this chapter, the concepts of sliding mode control are discussed elaborately. These basic concepts are essential to understand the controller design. The design of the controller is deliberately explained in chapter 7. The concept of higher order sliding mode and second order sliding mode control is studied and implemented effectively. The controller design is mainly based on traditional and second order sliding mode control algorithms, namely super-twisting control, is exemplified in this chapter. Gain adaptation of higher order sliding mode control is also elucidated, in order to be cognizant of estimating boundaries and assigning the gain values accordingly. Henceforth, enabling the fuel cell system to adapt to the disturbances and control them effectively without any flaw.

References:

[1] R.O'Hayre, S-W.Cha,W.Colella,F.B. Prinz, *Fuel Cell Fundamentals*, Wiley, 2006, ISBN 0-471-74148-5

[2] J. Larminie and A. Dicks, *Fuel Cell Systems Explained*, 2nd ed. New York: Wiley, 2003.

[3] C. Kunusch, "Second order sliding mode control of a fuel cell stack using a twisting algorithm," M.S. thesis, Electr. Dept., Nat. Univ. La Plata, Argentina, Mar. 2006.

[4] J. Pukrushpan, A. Stefanopoulou, and H. Peng, "Control of fuel cell breathing," *IEEE Control Syst. Mag.*, vol. 24, no. 2, pp. 30–46, Apr. 2004.

[5] G. Bartolini, A. Ferrara, and E. Usai, "Second order VSC for non linear systems subjected to a wide class of uncertainty conditions," in *Proc. IEEE Workshop Variable Structure Syst.*, 1996, pp. 49–54.

[6] A. Levant, "Sliding order and sliding accuracy in sliding mode control," *Int. J. Control*, vol. 58, no. 6, pp. 1247–1263, 1993.

[7] L. Fridman and A. Levant, "Higher Order Sliding Modes," in *Sliding Mode Control in Engineering*. New York: Marcel Dekker, Inc., 2002, ch. 3, pp. 53–101.

[8] L. Fridman and A. Levant, *Robust Control Variable Structure and LyapunovTechniques*. London, U.K.: Springer Verlag, 1996, ch. 1, pp. 106–133, no. 217.

[9] J. Pukrushpan, A. Stefanopoulou, and H. Peng, *Control of Fuel Cell Power Systems*. London, U.K.: Springer, 2004.

[10] A. Sabanovic, L. M. Fridman, and S. Spurgeon, *Variable Structure Systems:From Principles to Implementation.* London, U.K.: IEE, 2004.

[11] S. Spurgeon and R. Davies, "A nonlinear control strategy for robust sliding mode performance in the presence of unmatched uncertainty," *Int. J. Control*, vol. 57, no. 5, pp. 1107–1123, 1993.

[12] H. Sira-Ramirez, "Differential geometric methods in variable structure control," *Int. J. Control*, vol. 48, no. 5, pp. 1359–1390, 1988.

[13] V. Utkin, J. Gulder, and J. Shi, *Sliding Mode Control in Electro-Mechanical Systems*, London, U.K.: Taylor and Francis, 1999

[14] I. Matraji, S. Laghrouche and M. Wack, "*Second order Sliding Mode Control for PEM Fuel Cells*"49th IEEE Conference on Decision and Controls, Atlanta, GA, USA, 2010, pp.2765-2770.

[15]Y. Zhang, B. Zhou, "*Modeling and Control of a portable proton exchange membrane fuel cell-battery power system*", Journal of Power Sources,doi:10.1016/j.jpowsour.2011.05.022

[16]J. Correa, F. Farret, L. Canha, and M. Simoes, "*An Electrochemical-Based Fuel- Cell Model Suitable for Electrical Engineering Automation Approach*",Vol.51,NO.5,October 2004

[17] Y. Shtessel, F. Plestan, and M. Taleb, "Lyapunov design of adaptive super-twisting controller applied to a pneumatic actuator," *Proceedings of IFAC World Congress*, Milan, Italy, August 2011.

[18] T. Azib, R.Talj, O.Bethoux, and C.MarchandMember,IEEE. *"Sliding Mode Control and Simulation of a Hybrid Fuel-Cell Ultra capacitor Power System"*, 3425-3430,2010.

[19]M. Ghanes, M.Hilairet,J-P Barbot,O.Bethoux, *"Singular Pertubation Control for Coordination of converters in a fuel cell system"*

[20] SIRA-RAMIREZ,H: '*Sliding Motions in bilinear switched networks',IEEE Trans. On Circuits and Systems,* 1987,34(8),pp.919-933

[21] Venkatraman,R.,Sabanovic,A., and CukS.: '*Sliding Mode Control of DC-DC converters*', *Proceedings IECON 1985*, San Francisco,1985,pp.251-258

[22] Bilalaovic,F., Music,O., and Sabanovic,A.: *' Buck Converter regulator operating in Sliding Mode' . Proceedings 7thInternational Power Conversion Conference (PCI)*,Orlando,1983, pp331-340

[23]Nicolas,B., Fadel, M., and Cheron, Y.: '*Sliding Mode Control of dc-dc converters with input filter based on the Lyapunov-function approach'. Proceedings of European Power ElecronnicsConference(EPE)*, Seville, 1995, pp.1338-1343

[24] Rong-Jong Wai and Li-Chung Shih, '*Design of Voltage Tracking Control for DC–DC Boost Converter Via Total Sliding-Mode Technique'*,IEEE TRANSACTIONS ON INDUSTRIAL ELECTRONICS, VOL. 58, NO. 6, JUNE 2011

[25] AsifSabanovic, Leonid M.Fridman, Sarah Spurgeon.: *' Variable Structure Systems: from principles to Implementation'* Chapter 12, pg.265-293

[26] Huang, Y.-J., Kuo, T.-C., and Chang, S.-H. (2008), "*Adaptive Sliding Mode Control for Nonlinear Systems with Uncertain Parameters*", IEEE Transactions on System, Man, and Cybernetics

[27] Lee, H., and Utkin, V. I. (2007), "*Chattering Suppression Methods in Sliding Mode Control Systems*", Annual Reviews in Control.

[28] Plestan, Franck. Shtessel, Yuri. Bregeault, Vincent. Poznyak, Alexander. (2010)."*Adaptive sliding mode control for a class of MIMO nonlinear systems application to an electropneumatic actuator*"

[29] Plestan, F. Shtessel, Yuri. Bregeault, Vincent. Poznyak, A. (2010). "*New methodologies for adaptive sliding mode control*"

[30] A. Levant, '*Sliding order and sliding accuracy in sliding mode control*',International Journal of Control, 58,pp.1247-1263,1993